EXPERIMENTAL INVESTIGATION OF HEAT TRANSFER AUGMENTATION IN A CONCENTRIC TUBE HEAT EXCHANGER

A Project Report Submitted

in Partial Fulfillment of the Requirements

for the Degree of

Master of Technology

by

P. Suresh Kumar

Roll No. 01410315

DEPARTMENT OF MECHANICAL ENGINEERING

INDIAN INSTITUTE OF TECHNOLOGY, GUWAHATI

December, 2002

C E R T I F I C A T E

It is certified that the work contained in the thesis entitled **"Experimental Investigation of Heat Transfer Augmentation in a Concentric Tube Heat Exchanger",** by **P. Suresh Kumar**, has been carried out under our supervision and that this work has not been submitted elsewhere for a degree.

Dr. P. Mahanta
Assistant Professor
Dept. of Mechanical Engineering
I. I. T. Guwahati

Dr. A. Dewan
Associate Professor
Dept. of Mechanical Engineering
I. I. T. Guwahati

Dedicated to -

Sri. P. Gurumurty Rao

Smt. P. Mani

my parents for their love
and blessings

Smt P. Joty

my aunt for her love
and blessings

Late P. Chiti Amma

my grandmother for her love
and blessing

Smt. P. Sujata and Smt. P. Sarita

my sisters for their love
and encouragement

ACKNOWLEDGMENTS

After the completion of this Thesis, I experience feelings of achievement and satisfaction. Looking into the past I realize how impossible it was for me to succeed on my own. I wish to express my deep gratitude to all those who have extended their helping hands towards me in various ways during my short tenure at IIT Guwahati.

It gives me immerse pleasure to express my deep sense of gratitude and hearty thanks to my guides Dr. Pinakeswar Mahanta and Dr. Anupam Dewan, for their invaluable guidance and constant encouragement. They have spent a lion's share of their valuable time with me and made me feel the real zest of research work. I am highly indebted to them for their untiring devotion and willingness.

I would like to express my sincere thanks to Prof. Anil D. Sahasrabudhe (H.O.D. Mechanical Engineering Department) for providing all the facilities needed during my project work. I am thankful to Dr. Anoop Kumar Dass for providing I. C. Engines lab for building the setup, and conducting the experiments. I am grateful to Mr D. K. Sarma (Workshop superintendent) for guiding me in many occasions and helping me with a lot of patience during the fabrication of setup. His friendly advise and help from workshop technicians in various stages of building is really unforgettable. I am thankful to Dr. S. V. Prabhu, Dr. U. K. Saha, Dr. M. K. Das and all other faculty members who have guided me at various stages of the entire course. I am also thankful to Mr. Pankaj Kalita (Project associate for sponsored project on biogas), Mr. Milan Kakati, Mr. Arun Kanti Das and Mr. Tarun Deka (Technical assistants for sponsored project on biogas) for there kind help during building of setup and experimentation. There patience and dedication during the entire research period is unforgettable.

I am thankful to Mr. Amal Kalita, Mr. Manabendra Pathak, Mr. Bimal Das, and all other technical and non-technical staff of the Mechanical Engineering Department for their help in carrying out this work. I am thankful to Dr. A. K. Das (Assistant Professor, Design Department) for his kind help to provide the necessary tools and material during my fabrication work. I am also thankful to A.S. Grinspan, Pintu Lal Sardar, Amaresh Dalal, Piyuesh Gupta and all other friends

for their cooperation and help during the entire program.

I am thankful to my parents and other family members for their whole-hearted support and constant encouragement towards the fulfillment of the degree.

Above all it is the Lord Jaganatah's mercy and will that made me stand at this juncture of my life.

P. Suresh Kumar

December, 2002 IIT Guwahati

ABSTRACT

Heat transfer with laminar flow has wide applications in various fields of engineering such as chemical industries, desalination plants, solar energy collectors, etc. Improvement in the heat transfer rate in existing heat exchangers becomes essential with increase in operational time of heat exchanger because of factors like fouling and scaling. Various techniques have been described in the literature to enhance heat transfer rate in heat exchangers. However, most of the studies are restricted to plain tubes of small hydraulic diameter. In most of the past studies the friction factor was correlated to Reynolds number. Since in a large hydraulic diameter pipe hydrostatic pressure is one major parameter in addition to Reynolds number, the prediction of friction factor using correlations based on Reynolds number only may deviate from reality for a large hydraulic diameter pipe.

In some applications, such as air liquefaction process, crude oil transport over large distance involves large diameter pipes demanding large amount of pumping power. Determination of accurate friction factor is essential for such devices. Hence there is a need for studying friction factor for large hydraulic diameter systems.

In the present project a flow visualization study has been conducted in a newly built Reynolds apparatus to understand the flow pattern with twisted tape and wire coil inserts. The objective of the present work is to study the behavior of fluid mechanics and heat transfer parameters in a large hydraulic diameter duct flow with and without twisted tape insert. A mathematical analysis for large hydraulic diameter duct flow is presented to correlate the friction factor as a function of Reynolds number and hydrostatic pressure. Based on the present mathematical analysis friction factor correlations were developed. These developed correlations have been tested with various fluid and duct sizes. For large kinematic viscosity fluid flow in a small hydraulic diameter duct with large values of Reynolds number, the presently developed friction factor correlations show good agreement with that available in the literature.

The thesis is organized in six chapters. It begins with the introduction where, first the need for research on heat transfer augmentation in a heat exchanger has been justified. Then augmentation techniques have been discussed. In Chapter 2 about 55 papers have been reviewed to present the developments in the heat transfer augmentation techniques. Based on the review, foundation for the present

study has been laid out. Chapter 3 deals with fabrication of experimental setup and the experimentation procedure followed in the present work. The flow visualization study is presented in Chapter 4. The results from the present work are discussed in Chapter 5. Conclusions and future scope are presented in Chapter 6.

• • •

Contents

List of Figures

Nomenclature

A	area of cross-section perpendicular to flow direction
a	dimensionless constant
b	dimensionless constant
c	dimensionless constant
D	diameter
f	friction factor
g	acceleration due to gravity
h	head of liquid or heat transfer coefficient
Jg	new dimensionless number (Jaga)
k	thermal conductivity
l	length measured along the flow direction
m	mass flow
Nu	Nusselt number
p	static pressure
Q	discharge
q	heat transfer rate
r	distance along the radial direction

Re	Reynolds number
T	temperature
t	time
V	average velocity of flow
v	velocity of flow
w	work
X	distance from the leading edge of the test section
Y	twist ratio (pitch of the twisted tape/hydraulic diameter)

Greak Symbols

Δ	difference
μ	coefficient of dynamic viscosity of fluid
ν	coefficient of kinematic viscosity of fluid
ρ	density of fluid
τ	shear stress

Subscripts

cv	control volume
h	hydraulic
hy	hydrostatic

i	inner
in	intial
∞	mean bulk
fi	final
l	loss
lo	local
lmb	local mean bulk
lw	local wall
o	outer
t	total
tt	twisted tape
w	wall

Superscripts

$\dot{}$	rate
$\ddot{}$	rate

Chapter 1

INTRODUCTION

Heat exchanger is a device facilitating heat transfer between two or more fluids. It is extensively used in several industries, such as thermal power plants, chemical processing plants, air conditioning equipment, refrigerators, radiator for space vehicles as well as automobiles etc. Heat exchanger has been classified in many different ways. A typical classification is given in Fig. 1.1.

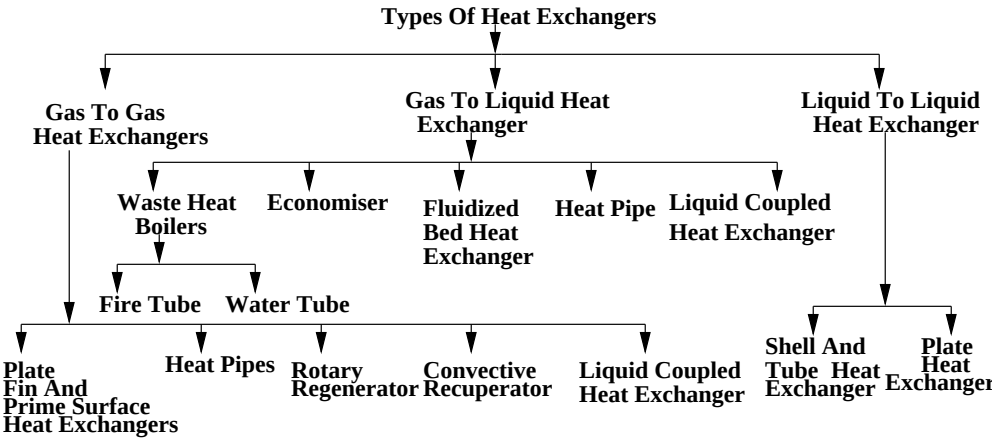

Figure 1.1: Classification of heat exchangers.

The design of heat exchanger is complicated, requiring a consideration of different modes of heat transfer, pressure drop, sizing, long term performance estimation as well as economic aspects. Most of the designs are based on compactness of the

unit. The compactness may be defined as the ratio of the heat transfer surface area on one side of the heat exchanger to the volume. Generally, a medium heat exchanger with a surface area density on any one side greater then 700 m^2/m^3 is referred to as a compact heat exchanger regardless of its structural design. As a heat exchanger gets older, the resistance to heat transfer rate increases due to fouling or scaling. This is particularly true in heat exchangers used in marine as well as chemical industries. Also in some industries there is a need to increase the heat transfer rate in the existing heat exchanger. Therefore to maintain the desired heat transfer in an existing heat exchangers several methods have been invented in the recent years and they are discussed in following sections.

1.1 Heat Transfer Augmentation

In recent years, high costs of energy and material have resulted in an increased effort aimed at producing more efficient heat exchange equipment through an augmentation of heat transfer. Techniques of heat transfer augmentation are relevant to several engineering applications. An heat exchanger for an ocean thermal energy conversion (OTEC) plant requires a heat transfer surface area of the order of $10,000$ m^2/MW. Therefore an increase in the efficiency of the heat exchanger through an augmentation technique may result in a considerable saving in the material cost. Desalination is another application in which large heat transfer surfaces are required and possibilities exist for the use of an augmented system. Some of the cases where heat transfer augmentation is desirable are:

1. Old heat exchangers subjected to fouling or scaling.
2. Heat transfer in fluids having low thermal conductivity, such as, air, various gases and oils.
3. Size limitation of heat exchangers in specific applications, such as, space vehi-

cles, automobile, etc, where the goal of the designer is to reduce the weight of the unit.

1.1.1 Augmentation Techniques

There are three different methods to enhance the heat transfer rate in a heat exchanger.

1. Active method
2. Passive method
3. Compound method

1.1.1.1 Active Method

As the name indicates, this method involves some external power input for enhancement of heat transfer. This method has not shown much potential due to:

1. Complexity in design.
2. External power is not so easily available in all applications.

Some examples of active methods are:

1. Induced pulsation by cams.
2. Induced pulsation by means of a reciprocating plunger.
3. Use of magnetic field to disturb the seeded light particles in a flowing stream.

1.1.1.2 Passive Method

This method involves no external power input. In this method additional power needed for heat transfer enhancement is taken from the available power in the system itself. This power utilized in enhancing heat transfer is known as the exergy

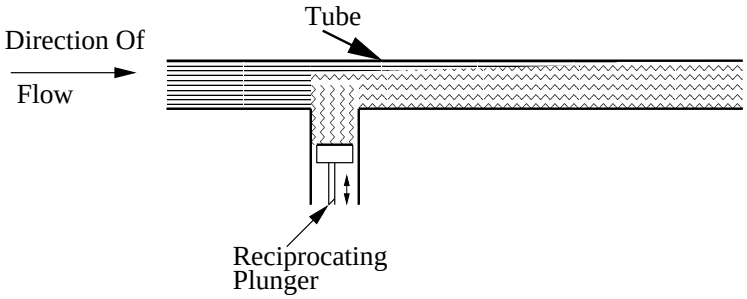

Figure 1.2: Active method with a reciprocating plunger.

loss. As is well known, the heat exchanger industry has been striving for improved thermal contact (enhanced heat transfer) and reduced pump power losses in order to improve the thermodynamic efficiency of heat exchanger. A good heat exchanger design should has a efficient thermodynamic performance, i.e, minimum generation of entropy or minimum destruction of available work (exergy) in the power/refrigeration system incorporating a heat exchanger. As we know, we can't stop exergy loss completely, but we can definitely minimize it through efficient design. Some of the examples of passive methods for heat transfer enhancement in heat exchangers are wire coil, twisted tapes, use of ribbed heat transfer surfaces, etc.

1.1.1.3 Compound Method

This method uses both active and passive method in a combination to take advantage of both the technique. It has to deal with a complex design, and hence has limited application.

1.1.2 Optimization

Usually an increase in heat transfer rate is accomplished by an increase in pressure drop. For example, in some situations the heat transfer coefficients are increased

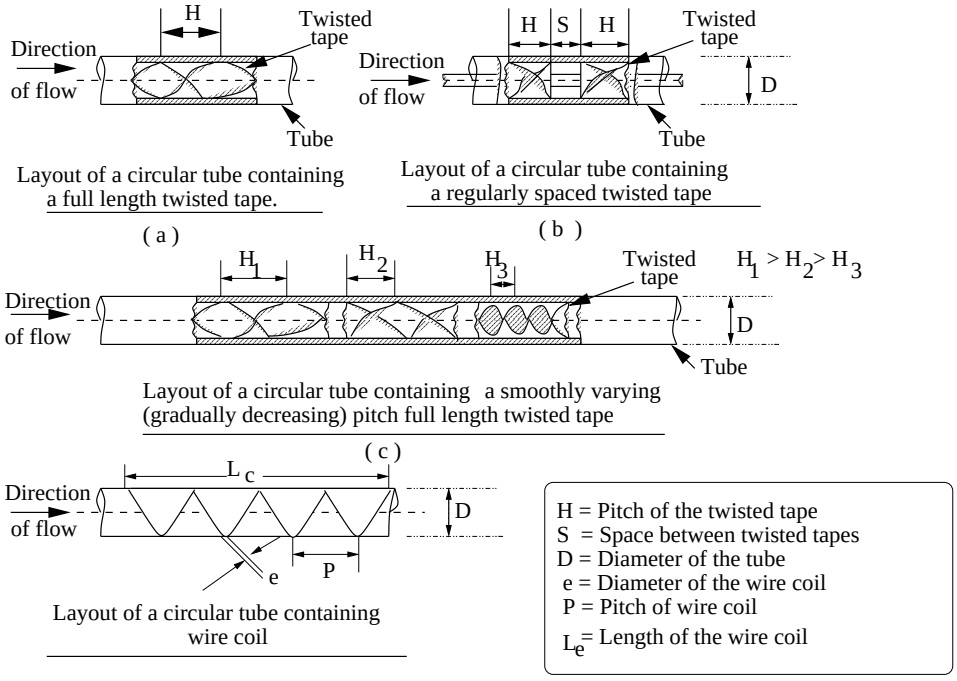

Figure 1.3: Different configuration for twisted tape and wire coil inserts.

at most about 4 times while the friction factor is increased as much as 50 times or more. An increased friction factor implies an increased power requirement for pumping the fluid. Hence it is equally important to reduce the frictional loss while increasing the heat transfer rate. The best technique would be the one that results in an optimum values of both the parameters.

Chapter 2

LITERATURE REVIEW

An extensive literature survey of all types of heat transfer augmentation techniques with external inserts has been discussed by Bergles [1]. In the present study twisted tapes and wire coils have been selected as an insert for heat transfer augmentation. Literature pertaining to twisted tape and wire coil inserts has been discussed in the following sections.

2.1 Heat Transfer Augmentation With Twisted Tapes

Witham [2] published his work on heat transfer enhancement by means of a twisted tape insert way back at the end of the nineteenth century. Since then reports on the new works have been pouring in continuously. The work on twisted tape first started with twisted tape inserts in circular ducts. Thereafter twisted tapes inserts have been used in non-circular ducts as well.

The width of the metal strip of twisted tape is equal to or less than the internal diameter of the duct depending upon whether the tape is loosely, snugly or tightly fitted inside the tube. The reduction in tape width causes a decrease in the pressure

drop and heat transfer rate. The twisted tapes may be extended all along the length of the duct and in this case tapes are called full length tapes. The tapes can be short length also when the tapes extend only up to certain length of the duct and there is a decaying swirl downstream of the tape. Twisted tapes can also be regularly spaced when the small pieces of tapes are welded on to the ends of a thin circular rod. Twisted tapes can be placed inside the duct by pitching as well. There can be splits at the edges of the tape or there can be holes punched on the tape surfaces. All these variations in a twisted tape are made to reduce the increased pressure drop usually accompanied by enhanced heat transfer rate. Investigators have also tried the compound use of twisted tapes and other means of passive heat transfer enhancement techniques.

Royds [3] found that a twisted tape performs better than a plain tube in terms of heat transfer even for the flow of low Prandtl number ($Pr < 1$) fluids. He further found that the tighter twist tapes provide an improved heat transfer rate at a cost of increase in pressure drop. Cresswell [4] noticed that the ratio of maximum velocity to mean velocity is smaller in case of swirl flow compared to that for a straight flow. Kreith and Margolis [5], Thorsen and Landis [6] observed that centrifugal force field aids convection when the fluid is heated up and inhibits convection when the fluid is cooled by pushing the heavier fluid particles outward and lighter fluid particles inward. Gambill and Bundy [7] found that twisted tapes are also important for higher Prandtl number fluids (e.g., ethylene glycol, etc). Smithberg and Landis [8] gave an analytical model of swirl-tape-generated swirl flow mechanism. Lopina and Bergles [9] observed that the difference between isothermal and heated flow friction factor for the swirl flow of liquids is substantially less than the corresponding difference for a plain tube.

The general conclusion from the aforementioned investigations and the works

of Colburn and King [10], Seigel [11] and Koch [12] is that, for turbulent flow, comparable increase in heat transfer coefficients are accompanied by pressure drops which are several orders of magnitude grater than the plain tube values. It has been observed from the works of Cilburn and King [10], Seymour [13], and Kreith and Soju [14] that short length twisted tapes (about 25 - 45 % of tube length) perform slightly better than the full length twisted tapes, indicating thereby the persistence of the swirl over a substantial part of the test section downstream of the tape.

In the early seventies Date [15] made a review of the available friction factor and Nusselt number results for flow in a tube containing a twisted tape and pointed out that the existing correlations deviate from the measurements by 30%. The studies by Kepper [16], and Kidd and Jr. [17] proved the usefulness of the twisted tapes in gas cooled nuclear reactor.

Date [18] formulated and solved numerically the problem of fully developed, uniform property flow in a tube containing a twisted tape. He compared the existing experimental data with his own numerical predictions. Bolla et. al. [19] observed that transverse rib perform better than twisted tape insert in a duct flow. Zozulya and Shkuratov [20] found that smooth decrease of pitch of a twisted tape does have significant influence on the heat transfer. Huang and Tsou [21] studied free swirl flow in pipes. Blackwelder and Kreith [22] recommended that an optimum design of heat exchangers with tape induced swirl flow must consider a combination of continuous and decaying swirl flow. Blackshall and Landis [23] studied boundary layer characteristics of incompressible twisted-tape-generated swirl flow. Watanable et. al. [24] observed that maximum thermal stress appears near the piping connecting parts of the cover plate of the plate fin heat exchanger channels. Genis and Rautenbach [25] studied the thermo-hydraulic characteristics of high velocity water flow in short tubes with twisted-tape inserts. Budov et. al. [26] predicted the loss of

head due to hydraulic resistance in a twisted tape generated swirl flow. Beckermann and Goldschimdt [27] observed that, in addition to convection, radiative heat transfer from the relatively hot (1260^0 C) cross twisted tapes in the flueway of a water heater plays an important role in the heat transfer to the tube wall and this phenomenon cannot be neglected. Yamada et al. [28] made similar observations. Gupte and Date [29] measured and semi empirically evaluated friction and heat transfer data for twisted tape generated helical flow in an annulus. Filipak [30] made an experimental study of the twisted tape generated swirl flow in a vertical (contrary to the usual particle of horizontal) test section. Donevski and Kulesza [31] predicted the frictional losses from the combined effects of the axial and tangential boundary layer flow coupled with an additional vortex mixing effect. Rao [32] performed an experimental study of the augmentation of heat transfer in axial ducts of electrical machines. Fomina et. al. [33] checked the first pilot plant having economizers with twisted tape fins.

Algifri and Bharadwaj [34] and Algifri et. al. [35] presented a series of solutions to governing equations for short length twisted tape generated decaying swirl, which were deduced from the Navier-Strokes equations. Burfoot and Rice [36] found that the surface roughness of a twisted tape insert affects the thermohydraulic characteristics. Kumar and Bharadwaj [37] obtained theoretically the heat transfer and pressure drop correlations using the Kreith and Sonju [14] solution for the velocity vector which decays along the axis of the tube.

Kumar and Prasad [38] have investigated experimentally the performance of a twisted tape inserted solar water heaters. Fujita and Lopez [39] while doing experimental investigation, did not find any evidence of tape fin effects in the heat transfer characteristics of a snugly fitted stainless steel tape insert when compared to Teflon tape insert. AI-Fahed et. al. [40] have observed that there is an optimum

tape width, depending on the twist ratio and Reynolds number, for the best thermo hydraulic characteristics.

Saha et. al. [41] have shown that, on the basis of constant heat flux, regularly spaced twisted tape elements do not perform better than full length twisted tapes. Rao and Sastri [42], while working with a rotating tube with a twisted tape insert, observed that the enhancement of heat transfer offsets the rise in friction factor due to rotation. Manglik and Bergles [43] have combined correlations for laminar and turbulent flows into a single continuous equation. For an isothermal friction factor, the correlation describes most of the available data for laminar, transitional and turbulent flows within 10%. However, a family of curves is needed to develop correlation for Nusselt number, due to non-unique nature of laminar to turbulent transition. Sivashanmugam and Sundaram [44] and Agarawal and Raja Rao [45] also studied the thermo hydraulic characteristics of the twisted tape generated swirl flow. Peterson et. al. [46] experimented with high pressure (8 - 16 MPa) water as the test liquid in turbulent flow with low heat fluxes and low wall to fluid temperature differences typically for liquid-liquid heat exchangers.

Naumov and Semashko [47] and Naumov et al. [48, 49] used a mathematical model available for a adiabatic cross section to study the pulsed asymmetric heating of pipes by an external heat flux and calculated thermo-physical parameters of cooled pipes containing twisted tapes within the collector of deviated ions in the T-15 Tokamak injection system. Yokaya et. al. [50] demonstrated a novel use of twisted tapes in controlling the flow in the continuous casting mold and refining process. Klaczak [51] found the usefulness of the short-length twisted tapes. Hijikata et. al. [52], while carrying out experiments in a vertical test section, observed that the radiation between the pipe wall and the twisted tape increases the heat transfer rate by about 50%.

Saha and Dutta [53] explained that on the basis of constant pumping power and constant heat flux boundary condition short length twisted tapes are found to perform better than full length twisted tapes for tighter twists. Multiple twisted tapes perform nearly as good as a single twist. Friction factor and Nusselt number are approximately 15% lower for twisted tape with smooth swirl with the average pitch same as that for uniform pitch throughout twisted tape. The uniform pitch twisted tape performances better than the twisted tape with a gradually decreasing pitch. Saha and Dutta [54] used a test fluid with a high value of Prandtl number (Servo therm medium oil).

2.2 Heat Transfer Augmentation With Wire Coils

Inaba and Ozaki [55] showed that the turbulent flow induced by a wire coil enhances heat transfer even in the downstream of the wire coil. They developed empirical relations for Nusselt number as a function of Pr and $\frac{P}{e}$ (where P denotes pitch of the coil and e denotes diameter of the coil). Pressure drop is found to be proportional to the length of the wire coil. Both high heat transfer characteristics and small pressure loss can be obtained by utilizing the leading edge effect near the tube and the turbulent flow in the downstream of the wire coil. Among all the tested configurations $\frac{P}{e} = 10$ is found to be optimum for heat transfer enhancement with smaller pressure drop.

2.3 Objectives of the Present Study

In all the aforementioned studies the values of hydraulic diameter considered for study are small and the variation of friction factor was correlated to Reynolds number. Since in a large hydraulic diameter pipe, hydrostatic pressure is one major

parameter in addition to Reynolds number the prediction of friction factor using correlations based on Reynolds number only may deviate from reality for large hydraulic diameter pipe.

In the present project an analysis has been carried out for large hydraulic diameter annulus correlating the friction factor with Reynolds number and hydrostatic pressure. An experimental setup has been constructed for the study. Experiments were conducted in the fully developed region of a smooth circular pipe and an annulus with and without twisted tape insert. The variation of friction factor with Reynolds number and hydrostatic pressure has been studied. The variation of friction factor due to hydrostatic pressure for different fluids has been discussed. The Nusselt number variation in a large hydraulic diameter annulus for both with and without inserts has been studied.

Chapter 3

EXPERIMENTAL SETUP

The detail of the experimental setup design, fabrication, experimentation procedure and uncertainty involved in the present experimentation are discussed in the following sections.

3.1 Experimental Setup Description

The experimental setup designed and fabricated for the present study has been shown in Fig. 3.1. It consists of a concentric tube heat exchanger made of plexiglas with an inner diameter $D_i = 20\ mm$ and outer diameter of $D_0 = 50$ mm. The inlet to the heat exchanger is connected to a storage tank and the outlet is connected to a discharge tank Fig. 3.2. The storage tank is maintained at a constant head. The inner tube of the test section is made of galvanized iron (GI) pipe with outer diameter 20 mm and thickness 0.5 mm. A nichrome heater coil is inserted in this pipe to provide the necessary heat flux. The inner tube of the test section is insulated lengthwise by asbestos disks to prevent the heat transfer along the length of the tube. Further the heater coil is thoroughly insulated by means of the ceramic bids to avoid the electric short circuit in the test section (Fig. 3.3).

Figure 3.1: A view of experimental setup.

3.2 Design Considerations

A detailed deign and fabrication of the various components used in the present setup are discussed in the following subsections:

3.2.1 Design Based On Maximum Reynolds Number

The generalized Bernoulli's equation in a pipe with head loss can be written as:

$$\frac{\int_1^2 dP}{\rho} + \frac{v_2^2 - v_1^2}{2} + g(Z_2 - Z_1) + \frac{\dot{w}_{cv}}{\dot{m}} + h_l = 0 \tag{3.2.1}$$

where:

$\frac{\dot{w}_{cv}}{\dot{m}}$ = Work done by the control volume per unit of flowing mass.

h_l = Loss which accounts for the rate at which mechanical energy is irreversibly converted into internal energy.

Figure 3.2: Connection of heat exchanger to the inlet tank.

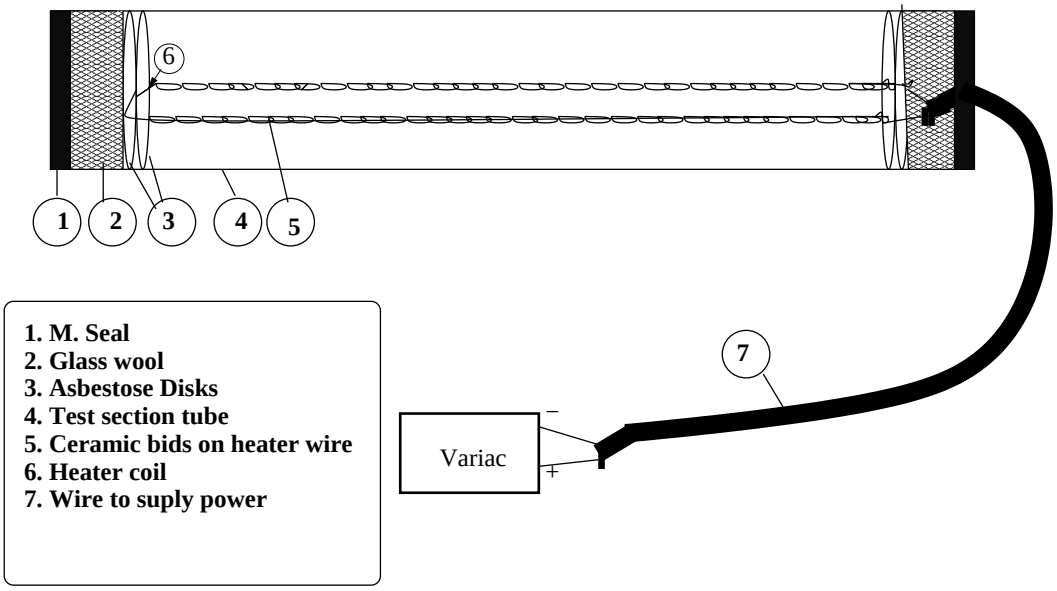

Figure 3.3: Inner pipe of the test section.

= Head loss + Friction work + Energy dissipation

$= \frac{4.f.L.V^2}{2.g} + \sum \frac{K.V^2}{2}$

= Pipe friction (Major loss) + Obstruction to flow (Minor loss).

In the present experiments both major and minor losses are important as the pipe length under consideration is small. All other notations in Eq(3.2.1) have their standard meanings. For the present study $\frac{P_2 - P_1}{\rho} = 0$ (As $P_1 = P_2 = P_{atm}$), $V_2 \gg V_1$ (as $\frac{V_1^2}{2}$ is negligible). $\dot{w}_{cv} = 0$ (as there is no work done by the control volume). Substituting all the above values in Eq(3.2.1),

$$\frac{v_2^2}{2} - gH + \sum \frac{4flv_2^2}{2D_h} + \sum \frac{K.v_2^2}{2} = 0 \tag{3.2.2}$$

Rearranging Eq(3.2.2),

$$H = \frac{v_2^2}{2g}(1 + \sum \frac{4fL}{D_h} + \sum K) \tag{3.2.3}$$

The hydraulic diameter for an annulus can be written as:

$$D_h = \frac{4 \times Cross\ sectional\ \ area}{Wetted\ perimeter}$$

$$= \frac{4 \times \frac{\Pi}{4}(D_2^2 - D_1^2)}{\Pi \times (D_2 + D_1)}$$

$$\Rightarrow D_h = D_2 - D_1 \tag{3.2.4}$$

where, D_2 = Inner diameter of the outer pipe, and D_1 = Outer diameter of the inner pipe. Reynolds Number

$$Re = \frac{v_2 D_h}{\nu} \tag{3.2.5}$$

$$\Rightarrow v_2 = \frac{Re\nu}{D_h} \tag{3.2.6}$$

Substituting Eq(3.2.4) and Eq(3.2.6) in equation Eq(3.2.3),

$$H = \frac{(\frac{\nu Re}{D_2 - D_1})^2(1 + \sum \frac{4.f.L}{(D_2 - D_1)} + \sum K)}{2g} \tag{3.2.7}$$

3.2.2 Hydraulic Entrance Length Calculation

As is well known that the internal flow is divided in two regions, namely developing region and developed region. In developing region, the velocity is function of both x and y coordinate (x- coordinate is in the direction of flow and y- coordinate is perpendicular to it). In the developed region, the velocity is not a function of x.

There are correlations reported in literature Ozisik [57] for the entrance length calculation of pipes. According to those correlations, the entrance length for a laminar flow is higher than that for the corresponding turbulent flow. Those correlations are as follows:

For laminar flow:

$$\frac{l_e}{D_h} = 0.06 \times Re \tag{3.2.8}$$

For turbulent flow:

$$\frac{l_e}{D_h} = 4.4 \times (Re)^{\frac{1}{6}} \tag{3.2.9}$$

Based on the above calculations it was found that outer diameter $D_0 = 50\ mm$, inner diameter $D_i = 20\ mm$ and total length of pipe $l = 4.5\ m$ will be suitable for the present experimentation. Large hydraulic diameter $D_h = 30\ mm$ has been selected to know the friction factor variation as a function of Reynolds number because almost all the aforementioned studies are restricted to small hydraulic diameter pipes only.

3.3 Components, Material And Fabrication

The manufacturing procedure of various components for the experimental setup is explained as follows:

3.3.1 Flange Design for Pipes Joints

The detailed design procedure for a flange design is available in Khurmi and Gupta [58]. The design correlations are as follows:

1. Nominal diameter of bolts, d=0.75t+10 mm, where t=thickness of the pipe
2. Numbers of bolts needed on a flange, n=0.0275D+1.6
3. Thickness of flange, $t_f = 1.5t + 3\ mm$
4. Thickness of flange, B=2.3d
5. Outside diameter of flange, D_0=D+2t+2B
6. Pitch circle diameter of bolts, D_P=D+2t+2d+12 mm
7. If strengthening of flange is required then ribs of thickness $t_r = \frac{t+t_f}{2}$ should be provided.

In the present setup the outer pipe has dimensions 60 $mm\ OD\ and$ 50 $mm\ ID$. Hence the flange that has been used has the following dimensions:

1. $d = 0.75 \times 5 + 10 = 13.75\ mm$
2. $n = 0.0275 \times 50 + 1.6 = 2.975 \approx 3$
3. $t_f = 1.5 \times 5 + 3 = 10.5\ mm$
4. $B = 2.3 \times 13.75 = 31.625\ mm$
5. $D_0 = 60 + 2 \times 31.625 = 123.25\ mm$
6. $D_P = 60 + 2 \times 13.75 + 12 = 99.5\ mm$

Plexiglas flanges were fabricated according to the design dimensions and they were first joined with the plexiglas pipes of the heat exchanger by means of a tight push joint. Later on chloroform was used as an adhesive to ensure a good strength at the joint. At the joint a mixture of M. Seal and Aerldide is used to ensure that there

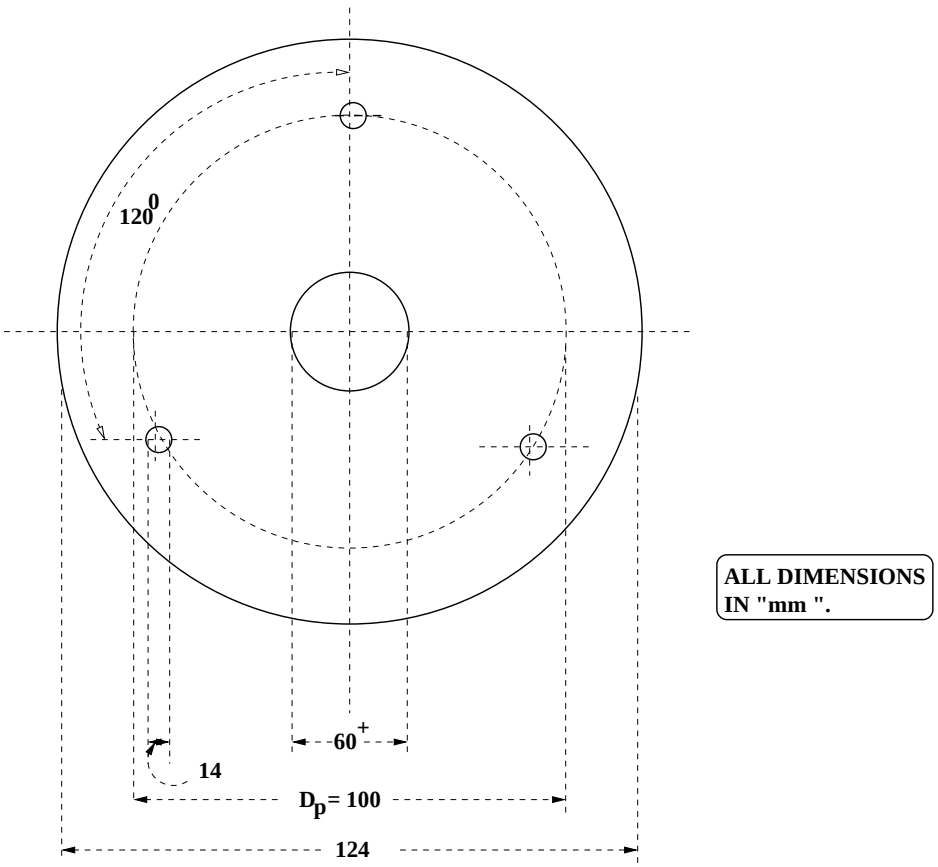

Figure 3.4: Flange Design.

is no leakage (Fig. 3.5). A rubber gasket is used to prevent the leakage through the flange coupling.

Figure 3.5: A view of flange coupling used for the heat exchanger pipes.

3.3.2 Fabrication of Components for Pressure Measurement

Cylindrical pressure taps of dimensions 7 mm outer diameter, 6 mm inner diameter, and 50 mm length were fabricated in the workshop. For the pressure tabs insert in to the heat exchanger pipes three holes of 7mm diameter were drilled to a depth of 0.25mm (half the pipe thickness, to prevent the disturbance in the flow due to pressure taps insert) circumferentially at six different streamwise locations, i.e, 1 m, 2 m, 3 m, 3.25 m, 4 m and 4.25 m from the inlet valve position. To prevent the fluctuation in the pressure drop reading cigarette filters were inserted in to the pressure taps. A vertical column manometer bank has been designed and fabricated to take the pressure readings at various pressure taps locations. Water with a small quantity of laser dye has been used as the manometer liquid in the present work. A view of the presently fabricated manometer setup is shown in Fig: 3.6. In the present work all readings are taken in the fully developed flow region only.

Figure 3.6: Manometer bank setup constructed in the present work to measure the pressure readings.

3.3.3 Components for the Temperature Measurement

The copper constanton thermocouples were used for the temperature measurement. The thermocouples are calibrated by conducting two different experiments. In both the case one junction of the thermocouple is placed in a constant temperature bath. Other end of the thermocouple is exposed to ambient condition in one experiment, and in the other experiment it is maintained at icepoint by placing it in a icebox. Using the experimental data a linear equation has been developed for temperature difference as a function of e.m.f. A plot for the comparison of developed linear equation data with the experimental data is shown in Fig. 3.7. From Fig. 3.7 it can be concluded that for both the test condition the equation data showing

good agreement with the experimental data. Hence this equation has been used to determine an unknown temperature. The thermocouples in the test section were connected with a multimeter by means of copper lead wires (Fig. 3.8) to measure the e.m.f across the thermocouples. A constant heat flux is supplied through a nichrome heater coil. The input heat flux is controlled by mens of a variac and the power input is measured by means of a wattmeter Fig. 3.9.

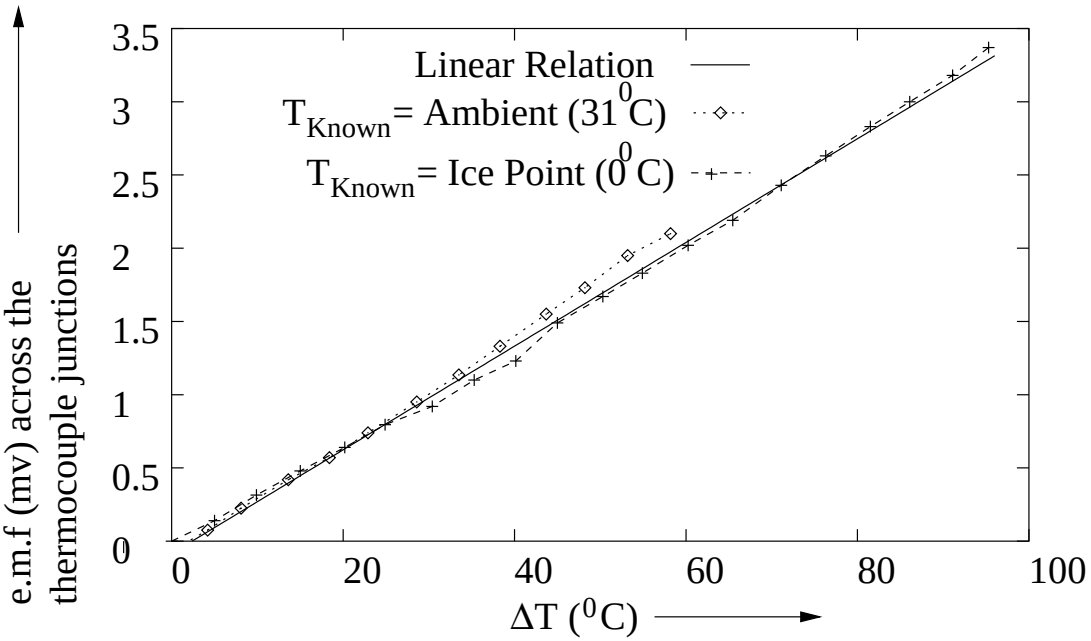

Figure 3.7: Thermocouple calibration.

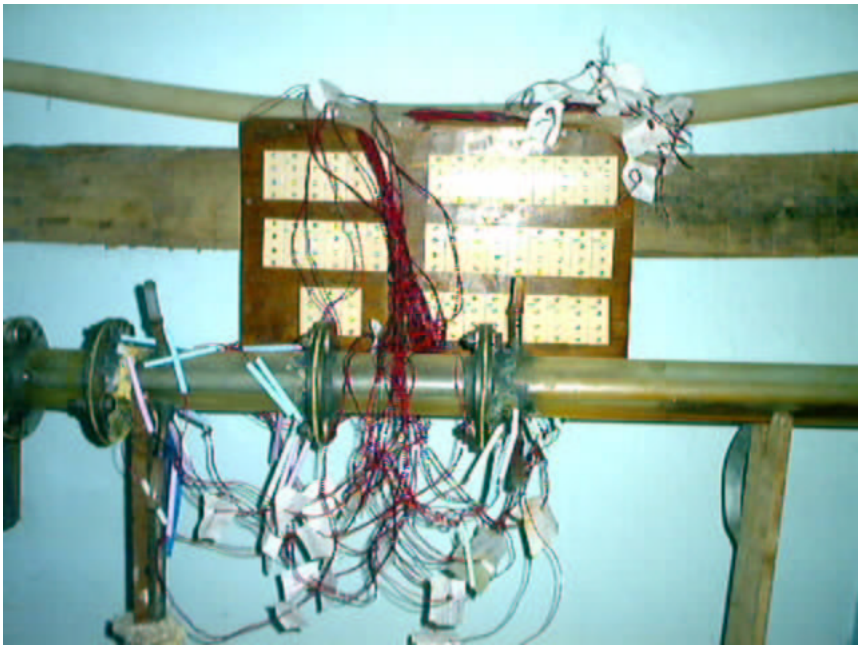

Figure 3.8: Test section

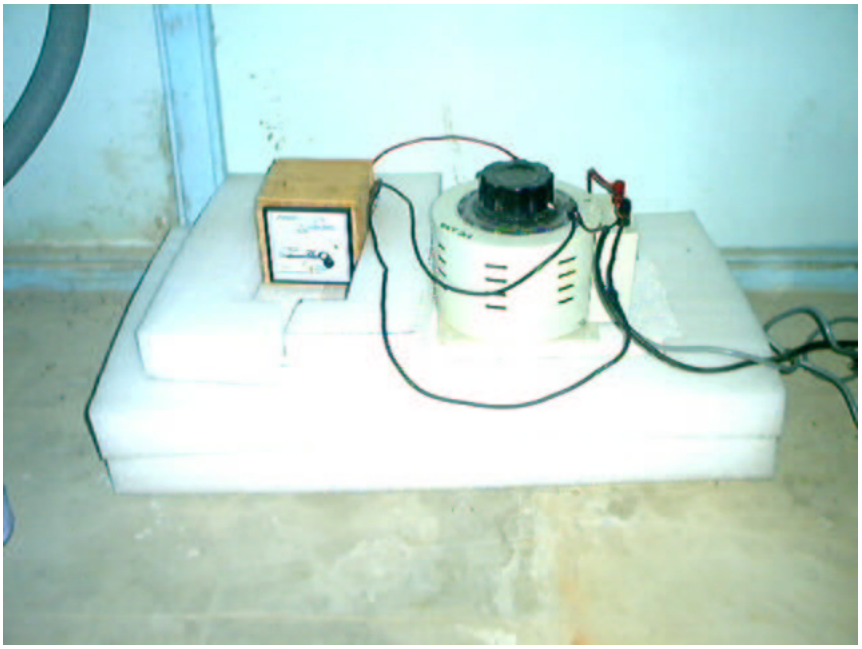

Figure 3.9: Power input control and measurement devices.

3.3.4 Fabrication of Heat Transfer Augmentation Equipment

Twisted tape was fabricated from the thin metal strips with smooth surface finishing (Fig. 3.10). The metal strips of width 14 mm, nearly equal to half the hydraulic

diameter of the annulus were attached to the ceiling by an attachment and twisted by applying the force from the bottom. Adequate load has been attached to the bottom of the twisted tape to avoid the bending of the metal strip during the twisting action.

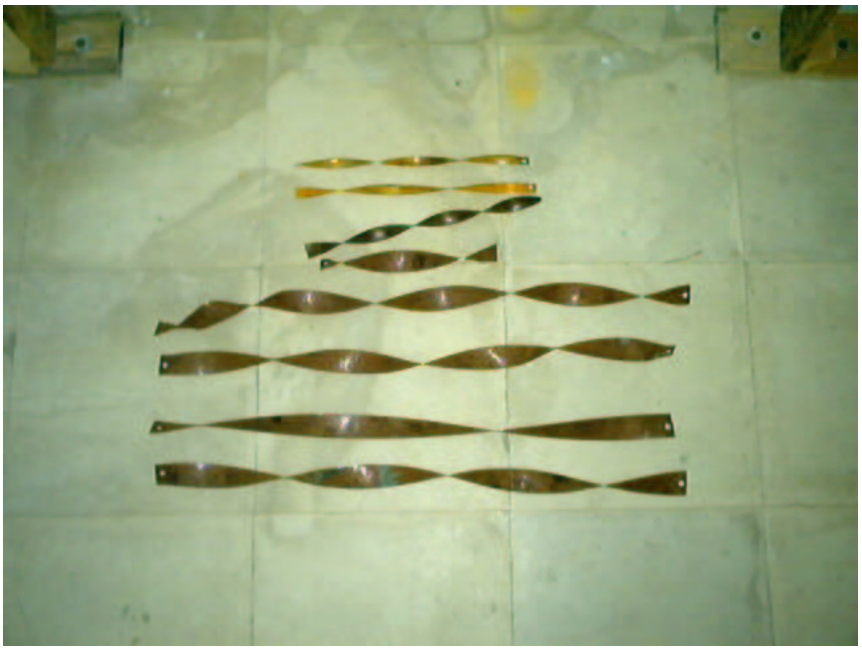

Figure 3.10: Twisted tapes fabricated for the present study.

3.4 Experimentation Procedure

Fig. 3.11 shows a schematic view of the experimental setup. An overhead tank with 0.2 m^3 capacity serves as a constant head reservoir and is used to discharge the test liquid to the test section through a regulating valve. The test section consists of concentric straight pipes made of plexiglas, which are joined at regular interval of 1.0 m by flanges. The inner diameter of the outer pipe is 50 mm and the annulus (flow passage) is of 30 mm in the radial direction throughout. The small pipe is supported inside the large pipe centrally by means of two small concentric cylinders made up of plexiglas of 0.3 mm thickness and 0.5 mm length (Fig. 3.11). This concentric cylinder is supported circumferentially in the large pipe at each 2 m distance by means of three thin pins of diameter 2 mm. The test section is kept horizontal by aligning it by means of a spirit level.

Pressure taps were placed at a distance of 4.0 m, 4.25 m and 4.75 m along the flow direction from the inlet valve position. At each location, three pressure taps were placed circumferentially at angles of 0^0, 120^0 and 240^0 measured from the top along the clockwise direction (Fig. 3.12). The pressure taps are 40 mm long and made up of cast iron (Fig. 3.13) with inner diameter of 8 mm and outer diameter of 10 mm. The joints of the pressure taps and the pipe are sealed with an adhesive to ensure no leakage. The pressure drop per unit length is found to be nearly same, i.e, $\frac{\Delta P_4 - \Delta P_4.25}{4.25-4} \approx \frac{\Delta P_4.25 - \Delta P_4.75}{4.75-4.25}$, hence it is concluded that the flow is fully developed.

All the pressure readings are taken under isothermal conditions. A U-tube manometer with water as working fluid is used for measuring the pressure drop at each probe location. The least count of the pressure measurement manometer is 0.5 mm. Water is used as the working fluid for the entire study. Water is supplied to the pipe from a big reservoir of capacity 700 liters, which is maintained at a constant

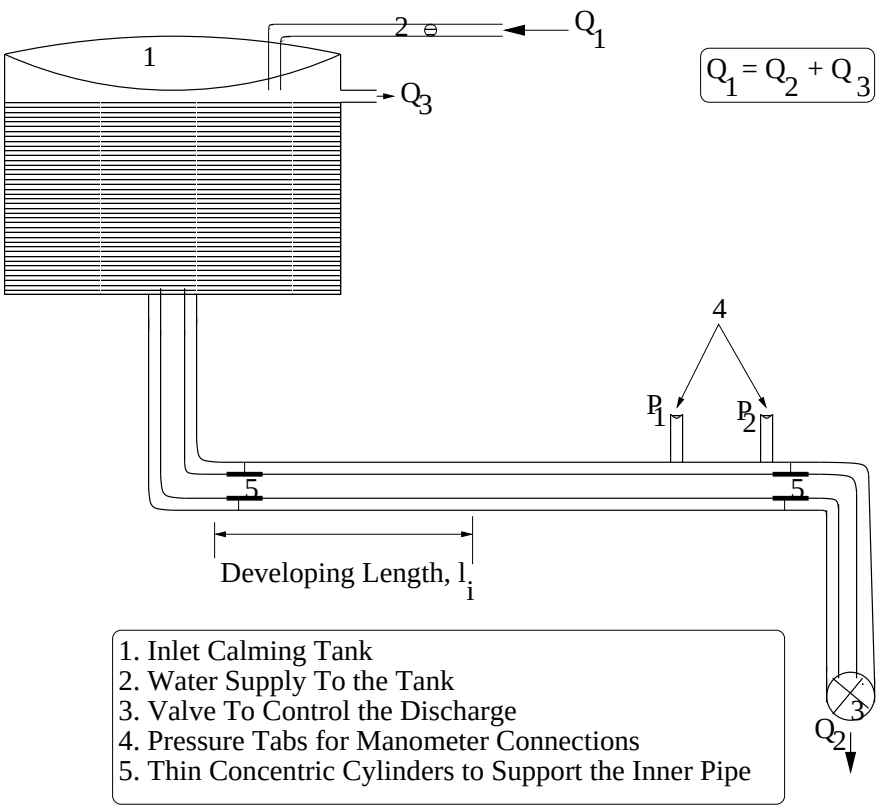

Figure 3.11: Schematic view of the experimental setup.

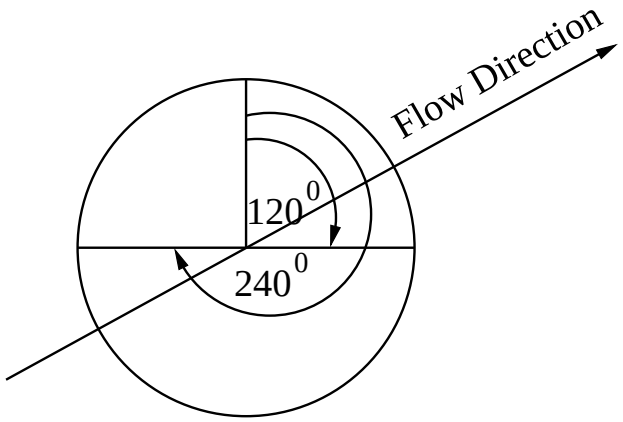

Figure 3.12: Angular positions for pressure taps, twisted tape, and thermocouple insert.

head. The discharge through the pipe is measured by means of a calibrated jar and stop watch.

Figure 3.13: Angular positions for pressure taps used in the present work.

Experimental data on pressure drop and discharge were collected under constant head conditions. At least two sets of data were collected to ensure the repeatability of the experiments. The average of the two sets of readings is used for analysis.

The developing length l_i for the laminar flow in an annulus is calculated using the following correlation Ozisik [57]:

$$l_i = 0.056 D_h Re \tag{3.4.10}$$

where Reynolds number $Re = \frac{V D_h \rho}{\mu}$. The friction factor f in the developed region is calculated from the average pressure drop readings of the three circumferential pressure taps at three streamwise locations (4.0 m, 4.25 m and 4.75 m from the inlet valve location) as given below,

$$f = \frac{2 h_l g D_h A^2}{l Q^2} \tag{3.4.11}$$

where h_l is the head loss noted from the manometer reading along the flow

direction, g is the acceleration due to gravity, D_h is the hydraulic diameter. A is the area of the cross section and Q is the flow discharge rate through the test section.

The ratio of the dynamic pressure to the shear stress produced by the velocity gradient due to the hydrostatic pressure variation along the radial direction in the test section is calculated as

$$Jg = \frac{\rho Q^2}{A^2 \mu \sqrt{\frac{g}{D_O}}} \tag{3.4.12}$$

where D_o is the inner diameter of the outer pipe in the annulus. In case of plain pipe, it represents the hydraulic diameter D_h.

The Reynolds number is calculated based on the discharge rate Q through the test section

$$Re = \frac{QD_h}{A\nu} \tag{3.4.13}$$

where ν is the kinematic viscosity of the working fluid.

The local value of the Nusselt number is calculated based on the difference between the local wall temperature T_{lw} and the local mean bulk fluid temperature T_{lmb}.

$$Nu = \frac{h_{lo} D_h}{k_{lo}} \tag{3.4.14}$$

where, h_{lo} and k_{lo} are the local heat transfer coefficient and local thermal conductivity of the fluid, respectively, at a thermocouple location. The local thermal conductivity k_{lo} of the fluid is calculated from the fluid properties [59] at the local mean bulk fluid temperature. The local heat transfer h_{lo} is calculated from the energy balance at a thermocouple location, i.e, $h_{lo}(T_{lw} - T_{lmb}) = q''$.

$$\Rightarrow h_{lo} = \frac{q''}{T_{lw} - T_{lmb}} \tag{3.4.15}$$

where, q'' is heat input q measured by the wattmeter per unit wetted area $\pi D_i l$, i.e, $q'' = \frac{q}{\pi D_i l}$. The length of the test section for the present experimental setup is $l = 0.5$ m.

Twisted tapes of two different twist ratios ($Y = 8.67$ and 9.23) were used. For the wall temperature measurement thermocouple were placed on the outer surface of the inner tube circumferentially at 0^0, 120^0 and 240^0 (Fig. 3.12) at three streamwise locations, viz. 0.02 m, 0.175 m and 0.375 m from the leading edge of the test section. Further for the measurement of mean fluid temperature thermocouples were placed at 0.0075 m and 0.015 m distance radially from the all aforementioned thermocouple locations.

Chapter 4

FLOW VISUALIZATION

Design and fabrication of inserts used in the experiments is a complex process. Twisted tape and wire coil inserts were selected for the study. In order to have a first hand information about the effect of these inserts prior to actual experiment, a flow visualization study was conducted. This study provided us information on the change in flow pattern when inserts were used.

To carry out the study, a Reynolds apparatus has been fabricated. In this apparatus water was used as a medium and ink was used as a dye. Four different types of twisted tapes (Y=4.5, 7.73, 10) and one wire coil were fabricated in the work shop. These inserts were tested in the Reynolds apparatus. Flow visualization has been conducted with each insert at three different locations, viz., at inlet, downstream and the outlet bend. Three values of Reynolds number (Re=108, 290 and 740) are considered for each study. Small values of Reynolds number is chosen for flow visualizing experiment because at higher values of Reynolds number the flow becomes turbulent throughout and reading the swirl flow is difficult. For each location, photographs have been taken by high speed digital camera as shown in the

following figures(4.1-4.12).

It is been found from the experiment that the twisted tape with a fine twist (Y=7.73) generates good swirl flow, from the heat transfer point of view for high values of Reynolds number. From study it is realized that with wire coil turbulent flow is achievable even in a laminar flow region, and the same flow pattern is found to be maintained in the downstream. The similar observation is recorded on the basis of pressure drop and heat transfer analysis by Inaba and Ozaki [55]. Hence wire coil can be used as an insert in a laminar flow region to improve the heat transfer rate significantly, even in the downstream. Fine twist twisted tapes maintaining good swirl motion even in the down stream and this may be reason that Saha and Dutta [53] found that a short length twisted tape with an intermediate twist ratio can give an improved heat transfer rate with a minimum pressure losses as compared to full length twisted tape.

This study is partial as it doesn't provide any information about the pressure drop, however these results eased the present investigation and helped a lot in selecting the the proper insert.

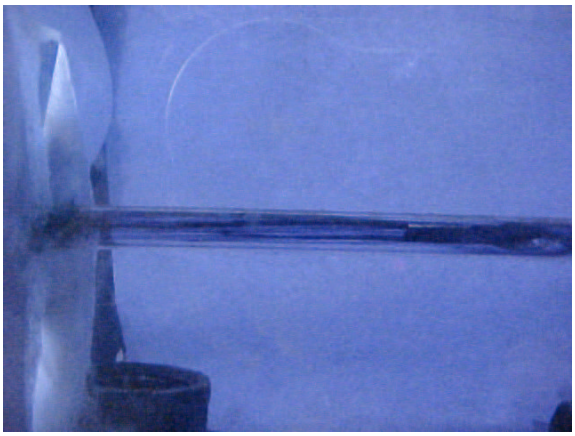

(a)

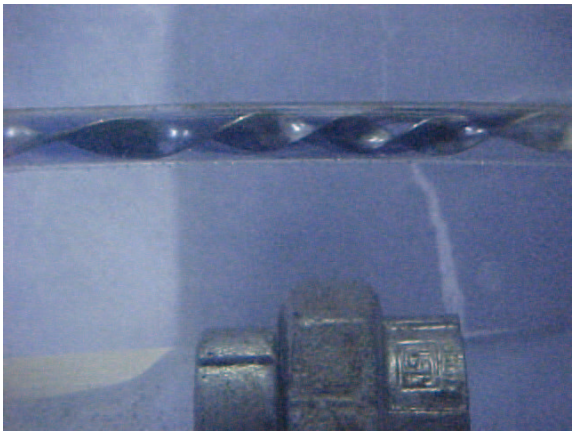

(b)

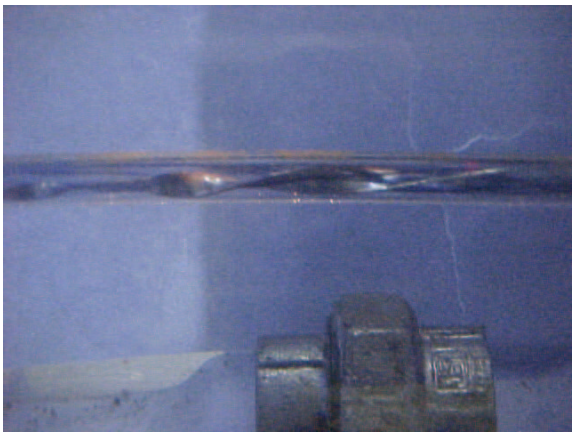

(c)

Figure 4.1: Tight twist (Y=4.5) inlet flow pattern (a) Re=108, (b) Re=290 and (c) Re=740.

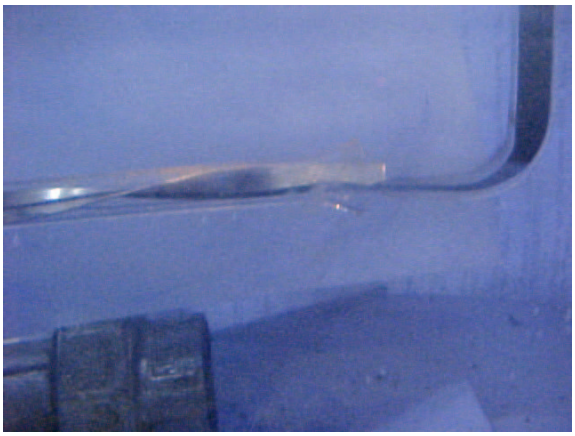

(a)

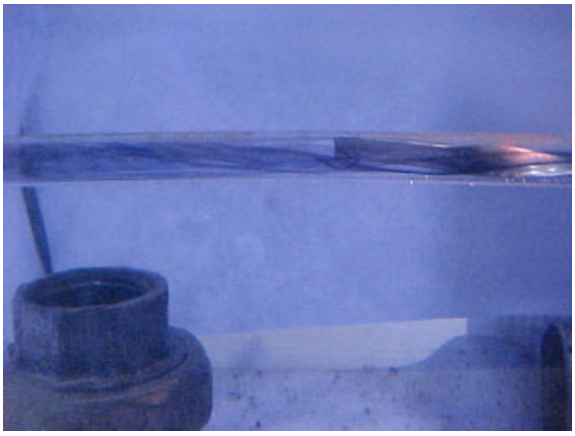

(b)

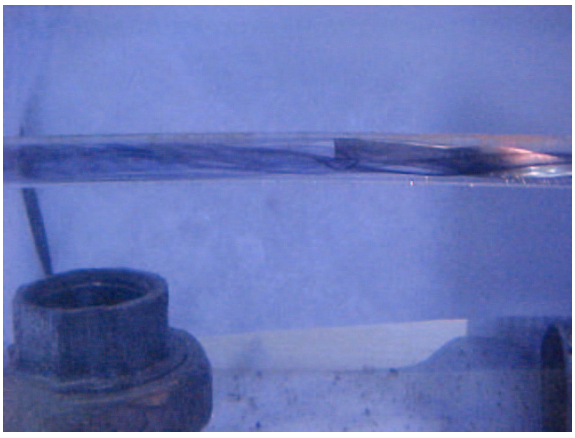

(c)

Figure 4.2: Lose twist (Y=10) inlet flow pattern (a) Re=108, (b) Re=290 and (c) Re=740.

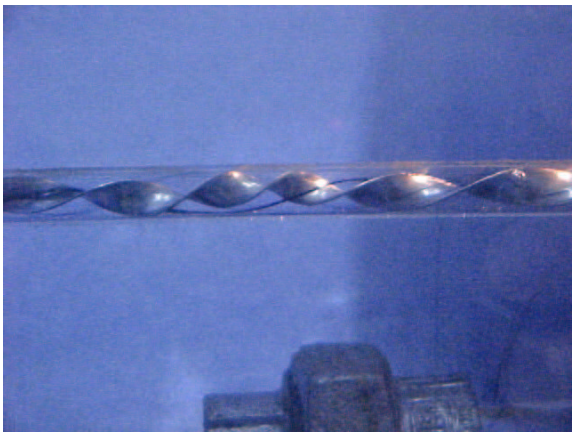

(a)

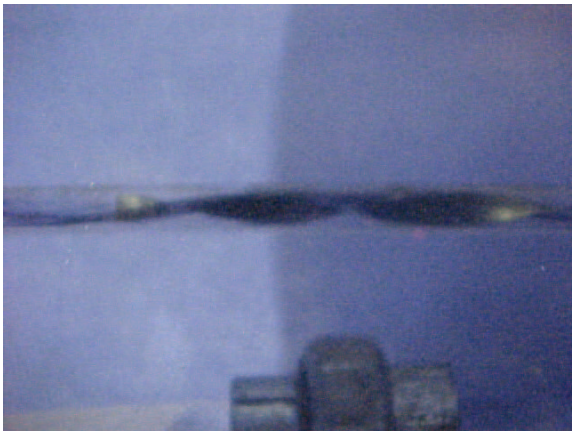

(b)

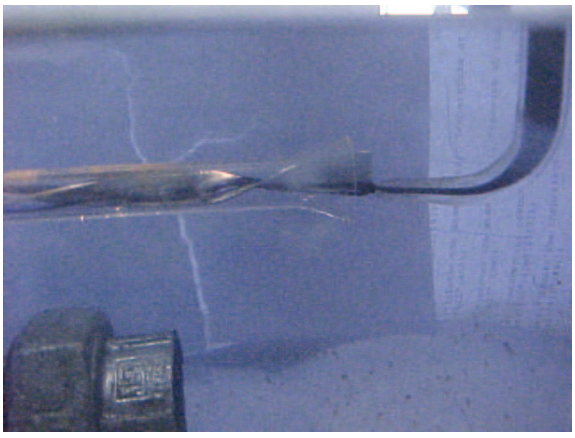

(c)

Figure 4.3: Fine twist (Y=7.73) inlet flow pattern (a) Re=108, (b) Re=290 and (c) Re=740.

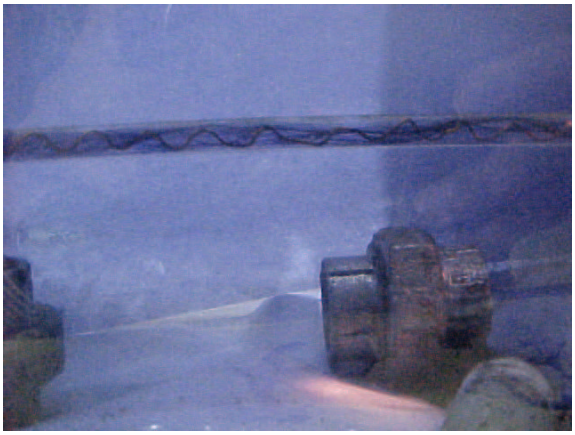

(a)

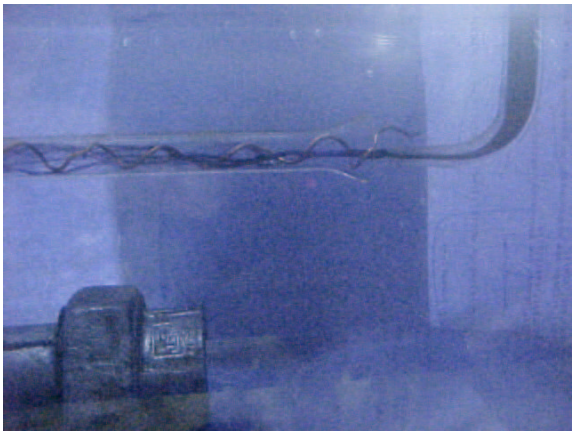

(b)

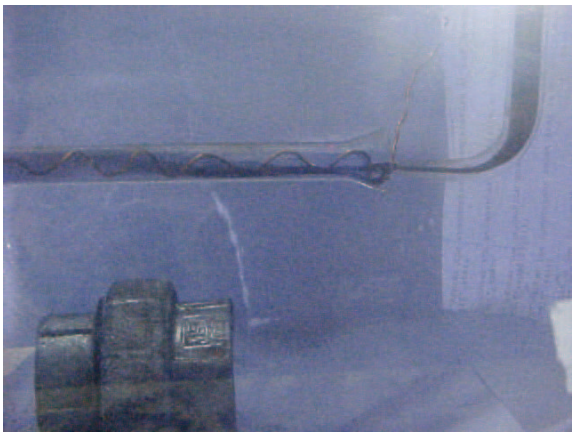

(c)

Figure 4.4: Inlet flow pattern for a wire coil (a) Re=108, (b) Re=290 and (c) Re=740.

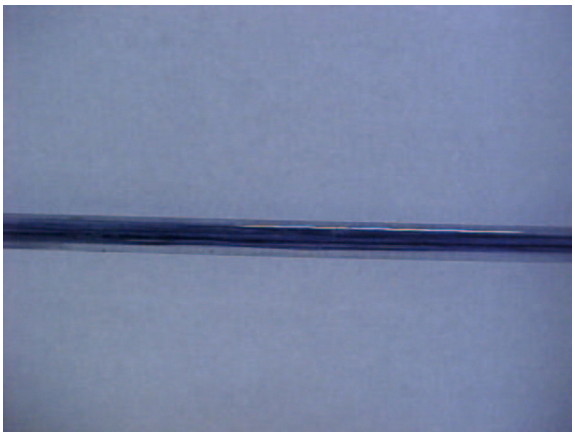

(a)

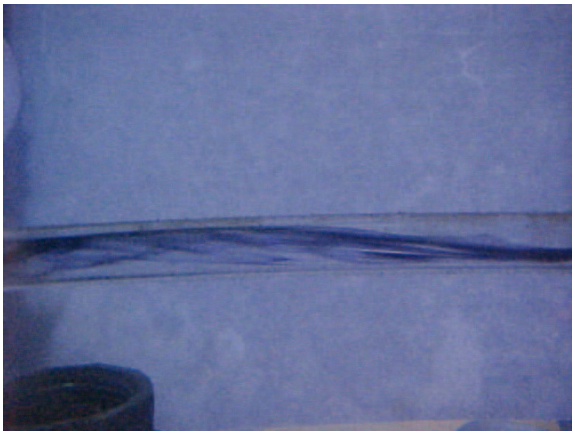

(b)

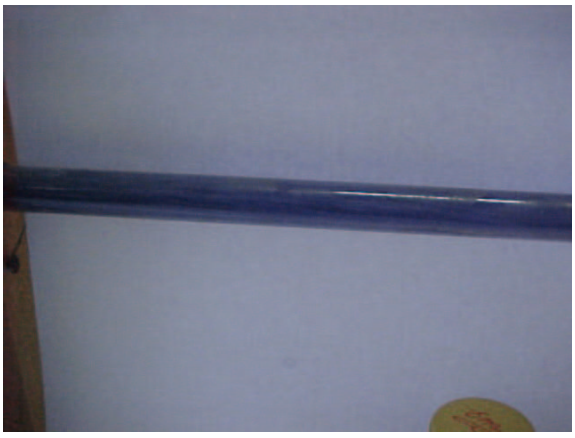

(c)

Figure 4.5: Tight twist (Y=4.5) downstream flow pattern (a) Re=108, (b) Re=290 and (c) Re=740.

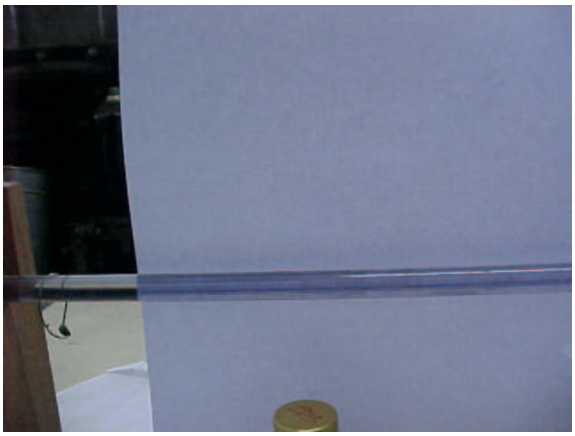

(a)

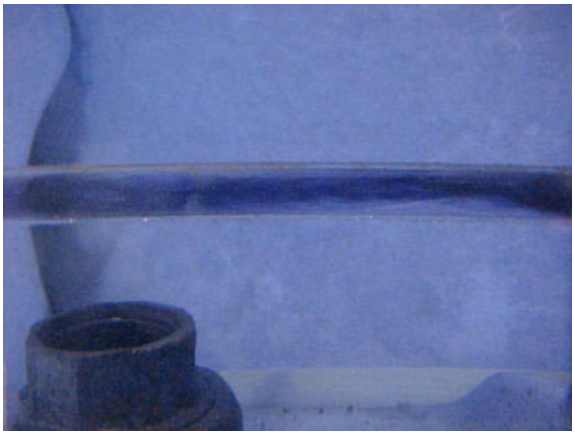

(b)

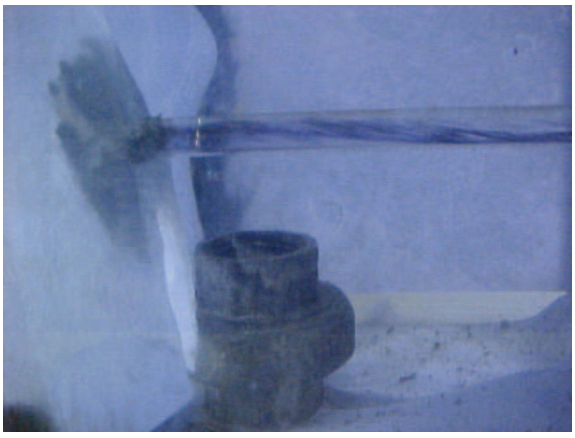

(c)

Figure 4.6: Lose twist (Y=10) downstream flow pattern (a) Re=108, (b) Re=290 and (c) Re=740.

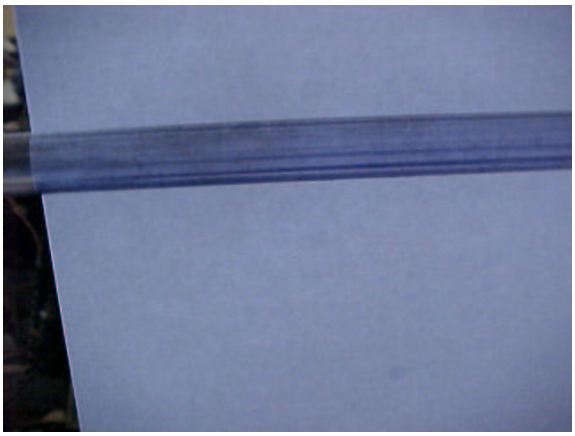

(a)

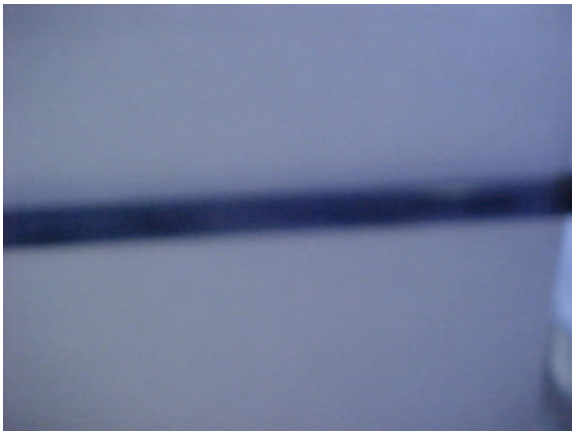

(b)

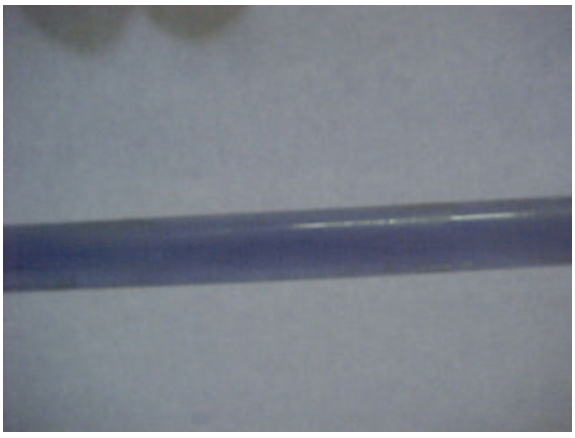

(c)

Figure 4.7: Fine twist (Y=7.73) downstream flow pattern (a) Re=108, (b) Re=290 and (c) Re=740.

(a)

(b)

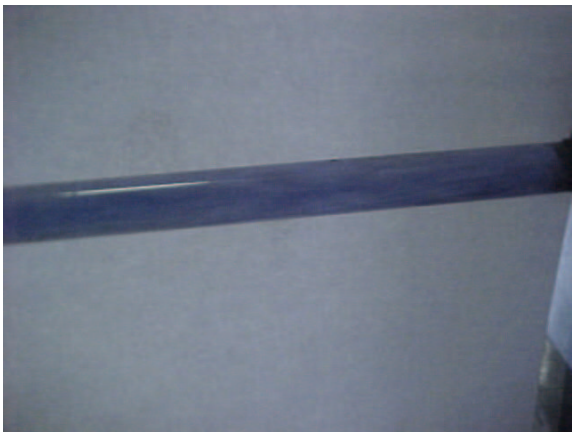

(c)

Figure 4.8: Downstream flow pattern for a wire coil (a) Re=108, (b) Re=290 and (c) Re=740.

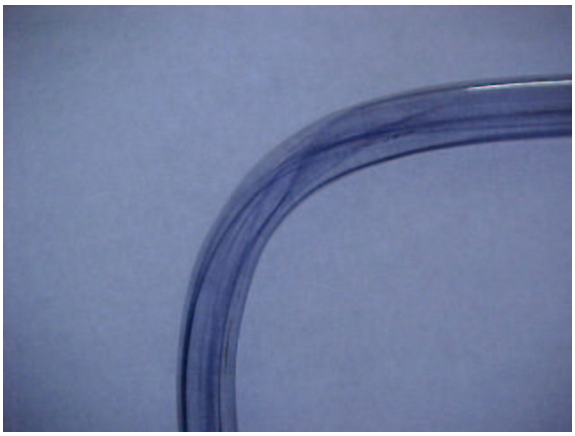

(a)

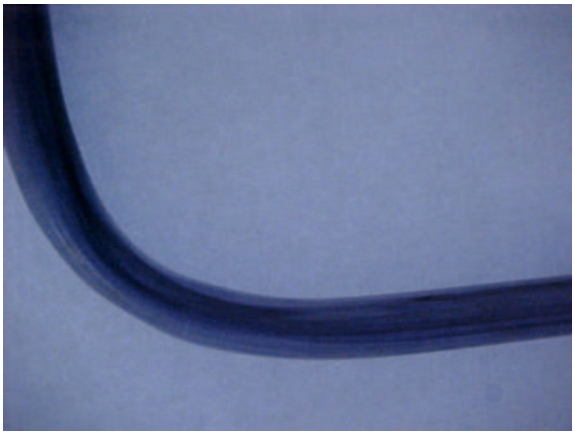

(b)

(c)

Figure 4.9: Tight twist (Y=4.5) flow pattern at bend (a) Re=108, (b) Re=290 and (c) Re=740.

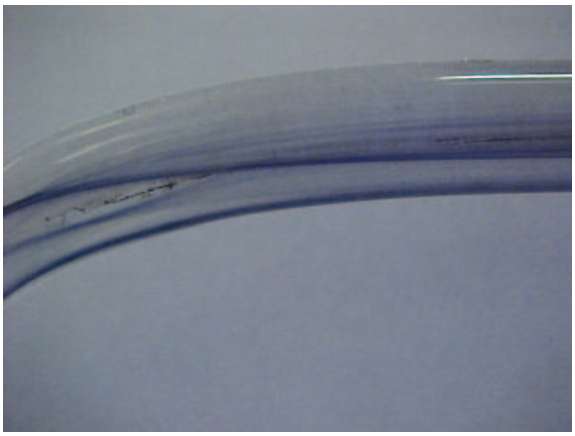

(a)

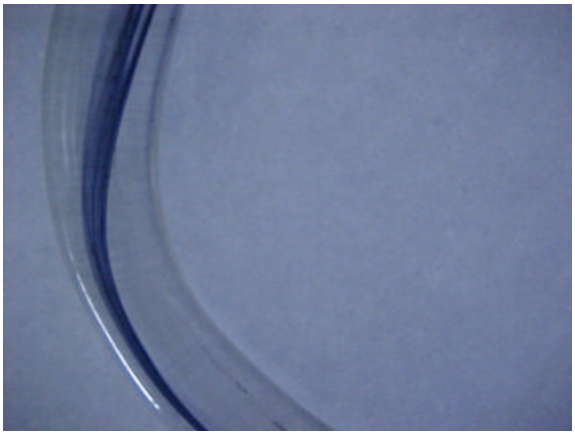

(b)

(c)

Figure 4.10: Lose twist (Y=10) flow pattern at bend (a) Re=108, (b) Re=290 and (c) Re=740.

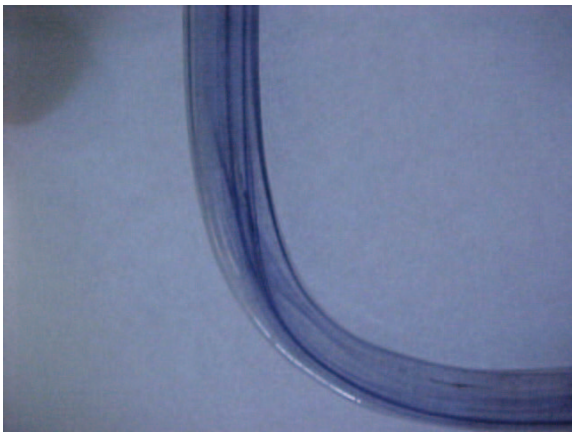

(a)

(b)

(c)

Figure 4.11: Fine twist (Y=7.73) flow pattern at bend (a) Re=108, (b) Re=290 and (c) Re=740.

(a)

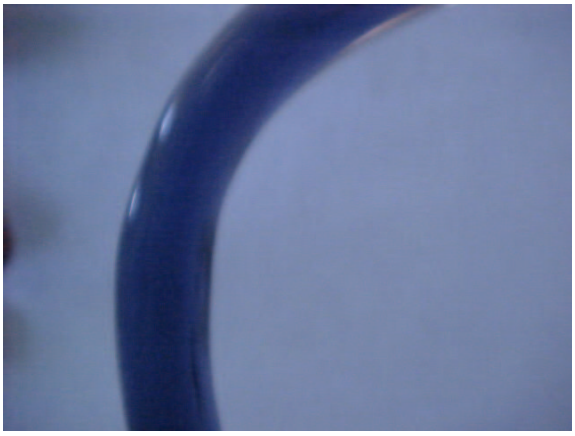

(b)

(c)

Figure 4.12: Flow pattern at bend for a wire coil (a) Re=108, (b) Re=290 and (c) Re=740.

Chapter 5

RESULTS AND DISCUSSION

5.1 Friction Factor Variation in Large Diameter Pipe and Annulus Without Insert

In the present investigation, it is observed that the pressure drop $\frac{\partial p}{\partial z}$ is a function of the wall friction only for small diameter pipes and liquids with large values of $\nu = \frac{\mu}{\rho}$. However, in a large diameter pipe ($D_h \geq 30\ mm$) with a liquid of small value of kinematic viscosity, the pressure drop is less dependent on the wall friction whereas it is strongly dependent on the hydrostatic pressure variation in the radial direction. The pressure drop due to the hydrostatic effect is negligible for the flow of a low density liquid in a small diameter pipe and hence generally it is neglected. But in the present study it is found that in a large diameter pipe and for a liquid with low kinematic viscosity this assumption can lead to a substantial error.

In order to simplify the analysis the Darcy's friction factor can be written as:

$$f = \frac{a\frac{\mu V}{D_h}}{\rho V^2} + \frac{b\mu\sqrt{\frac{g}{D_0}}}{\rho V^2} \tag{5.1.1}$$

where a and b are arbitrary dimensionless constants.

In the present investigation the hydraulic diameter chosen is quite large compared to that by Moody [55] and Olson and Wright [56]. The friction factor correlations presented by Moody [55] and Olson and Wright [56] are related to the Reynolds number.

The effect of hydrostatic pressure on friction factor is significant in the low Reynolds number range where the dynamic pressure is negligible as compared to the hydrostatic pressure. Mathematically Reynolds number can be written as:

$$Re = \frac{\rho V^2}{\mu\frac{V}{D_h}} \tag{5.1.2}$$

where ρV^2 is the dynamic pressure based on the average velocity and $\mu\frac{V}{D_h}$ is the shear stress due to wall friction based on the average velocity and the hydraulic diameter. The loss due to hydrostatic effect in ducts will increase with an increase in its characteristics length. In most of the earlier studies it was assumed that the results based on Reynolds number will be applicable for all sizes of pipes. This assumption in real practice will be erroneous for flow in a large diameter pipe. Hence to include the effect of hydrostatic pressure loss for the friction factor calculations a new number "Jg" is introduced in the present work. Jg is the ratio of the dynamic pressure based on the average velocity and head loss due to hydrostatic pressure based on the inner diameter of the outer duct for an annulus instead of hydraulic diameter because the variation of hydrostatic pressure along the radial direction in

an annulus depends on the inner diameter of the outer pipe. In the case of plane pipe Jg is simply based on the diameter of pipe. Mathematically

$$Jg = \frac{\rho V^2}{\mu\sqrt{\frac{g}{D_O}}} \tag{5.1.3}$$

Jg is similar to Reynolds number and the only difference is that the velocity gradient used in Reynolds number (Eq(5.1.2)) is shifted from $\frac{V}{D_h}$ to $\sqrt{\frac{g}{D_0}}$. In the present study it is found that number Jg can be used in combination with Re for all size of pipe, for accurate calculations of the friction factor. Eq(5.1.1) can be written in terms of the nondimensonal numbers as:

$$f_t = \frac{a}{Re} + \frac{b}{Jg} \tag{5.1.4}$$

where f_t is the total friction factor which is the sum of the wall friction factor and hydrostatic friction factor. The wall friction factor is dependent on the Reynolds number and can be written as:

$$f_w = \frac{a}{Re} \tag{5.1.5}$$

The hydrostatic friction factor is dependent on the newly introduced nondimensional number Jg and can be defined as:

$$f_{hy} = \frac{b}{Jg} \tag{5.1.6}$$

A series of experiments were carried out to study the variation of the friction factor with the Reynolds number as well as Jg. Correlations were developed for the friction factor as a function of Reynolds number and Jg. The correlation developed in the present investigation based on Jg and Reynolds number Re has shown good agreement with the existing results for small diameter pipes. The number Jg in the present investigation is found to be important for friction factor calculations in duct flows where the ratio of hydrostatic pressure to dynamic pressure is large.

In a small diameter pipe with a liquid of large kinematic viscosity the number Jg becomes negligible as the ratio of hydrostatic shear stress to the dynamic pressure head is negligible and hence f_{hy} is negligible as compared to f_w. But in a large diameter pipe with a liquid of small value of ν the number Jg is significant hence f_w is negligible as compared to f_{hy}. Further in the present work the effect of Jg on friction factor calculations for different fluids is studied using a correlation proposed in the present work.

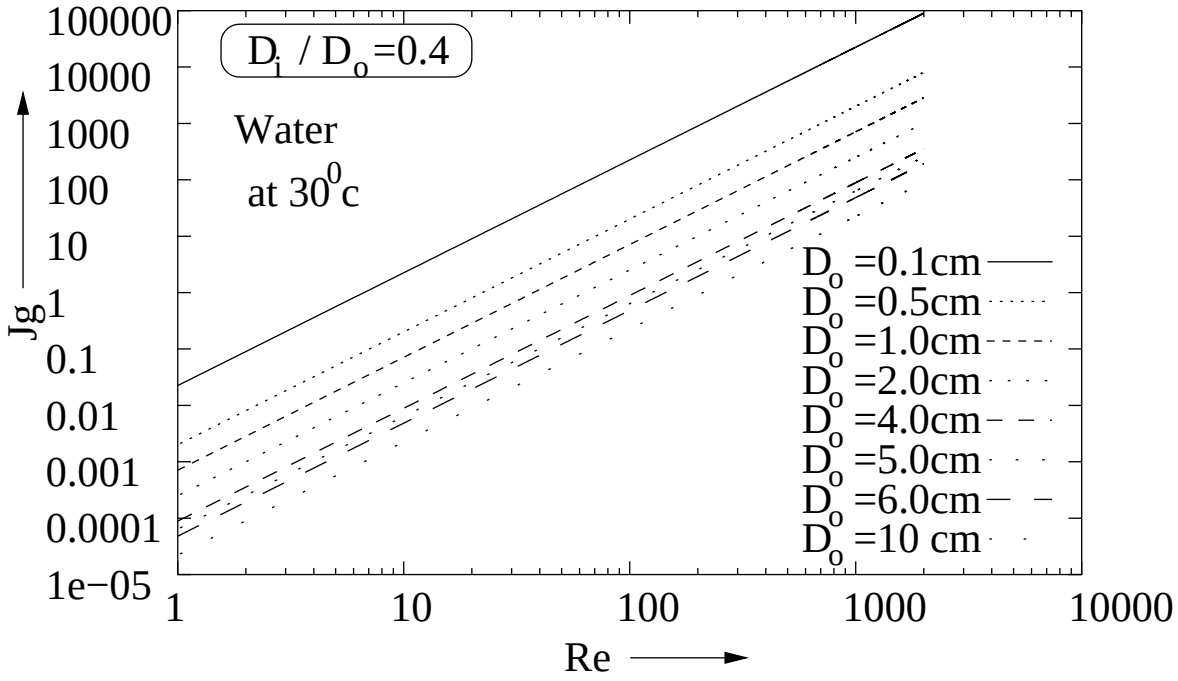

Figure 5.1: Variation of Jg with Re in an annulus.

To study the importance of hydrostatic effect in smooth pipe and annulus for different values of diameter and Reynolds number the variation of Jg with Reynolds number is plotted in (Figures. 5.1 and 5.2). Fig. 5.1 shows the variation of Jg with Reynolds number in an annulus for different values of diameter D_0 keeping the ratio same as that for the present experimental setup ($\frac{D_i}{D_0} = 0.4$). It can be seen that the number Jg increases linearly with Reynolds number. Further, Jg is large for small diameter pipe and large values of Reynolds number. The reason for this behavior is

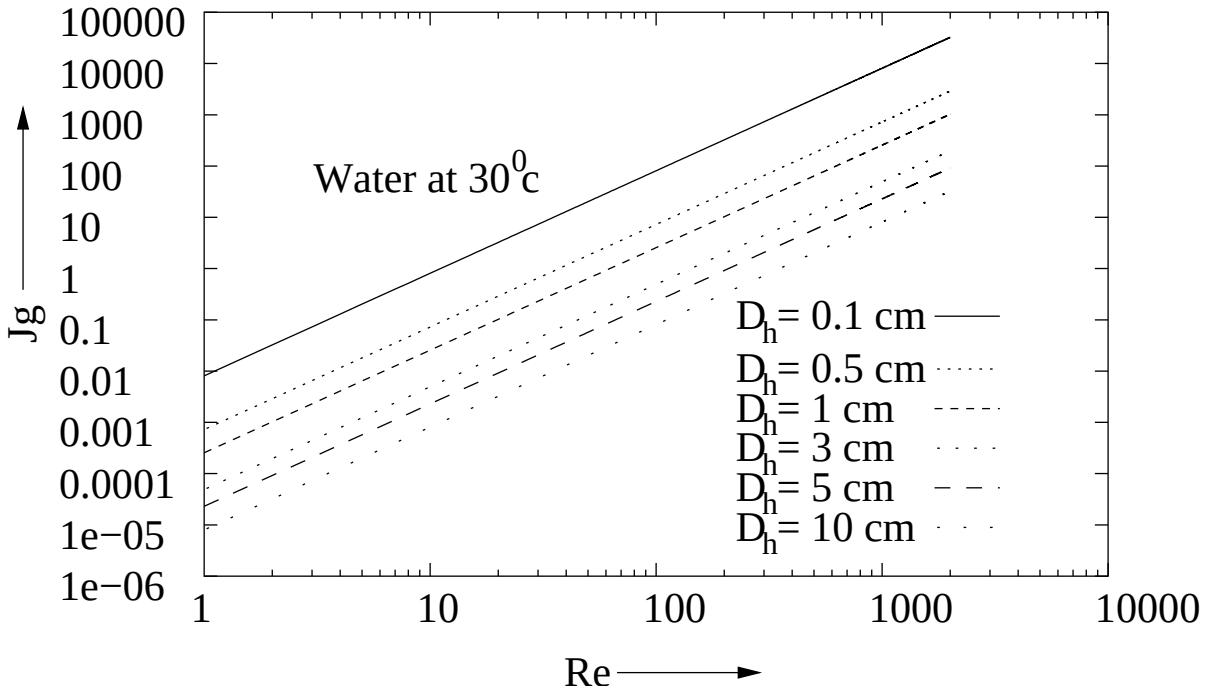

Figure 5.2: Variation of Jg with Re in a plane pipe.

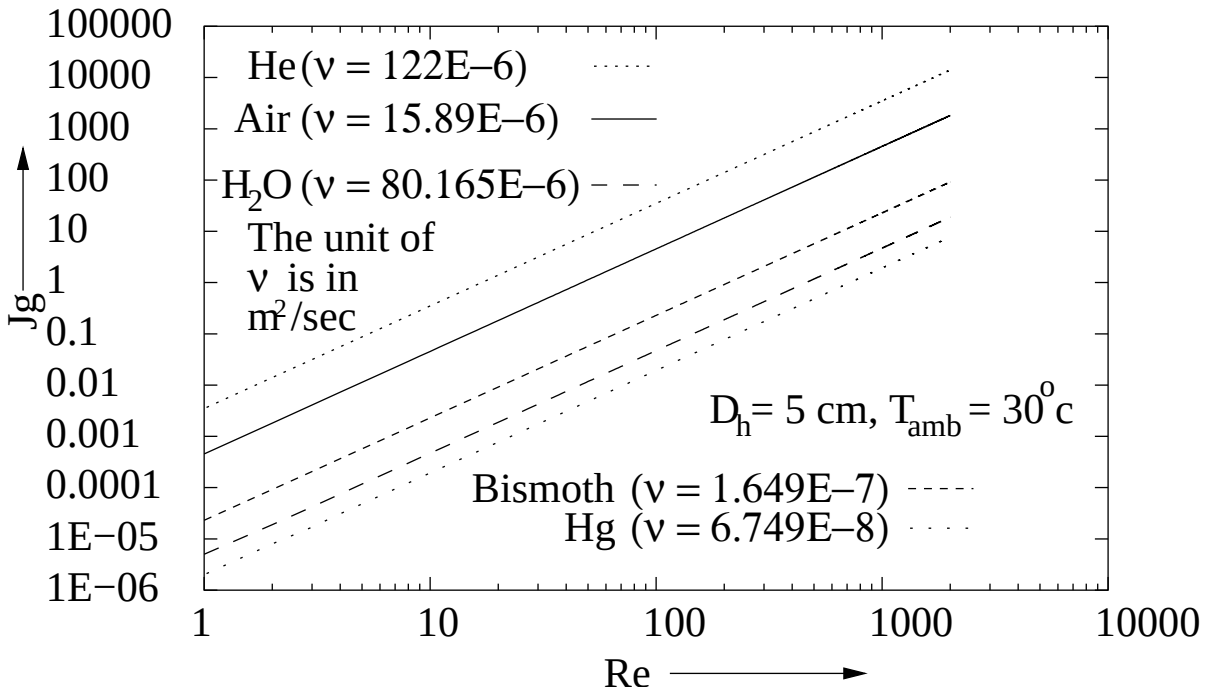

Figure 5.3: Variation of Jg with Re for different fluids in a plane pipe.

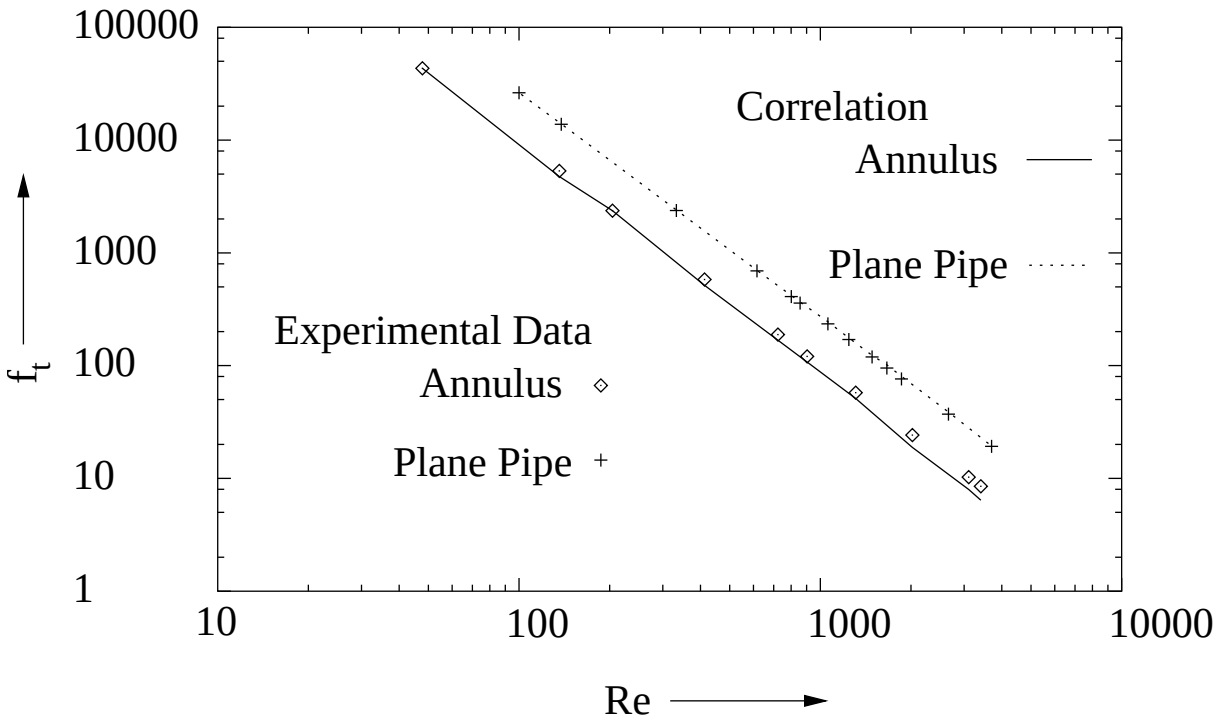

Figure 5.4: Variation of total friction factor f_t with Reynolds number Re in large hydraulic diameter pipe and annulus.

that in these cases the dynamic pressure is quite high as compared to the hydrostatic pressure. Hence the high dynamic pressure nullifies the shear stress effect due to the hydrostatic velocity gradient. Therefore according to Eq(5.1.4) the total friction factor will increase with an increase in the diameter of pipe and decrease in Reynolds number, due to a rise in the hydrostatic friction factor f_{hy} with a decrease of Jg. This is the reason that the present results do not match with that reported by Moody [55] and Olson and Wright [56] at low Reynolds number and large hydraulic diameter. The correlations developed in the present work yield values of friction factor in good agreement with those reported by Moody [55] and Olson and Wright [56] at high Reynolds number range and for small value of hydraulic diameter. Fig. 5.2 shows the variation of Jg with Reynolds number in a plane pipe, which is similar in nature to that for an annulus.

The variation of Jg with Reynolds number in a plane pipe for different fluids is

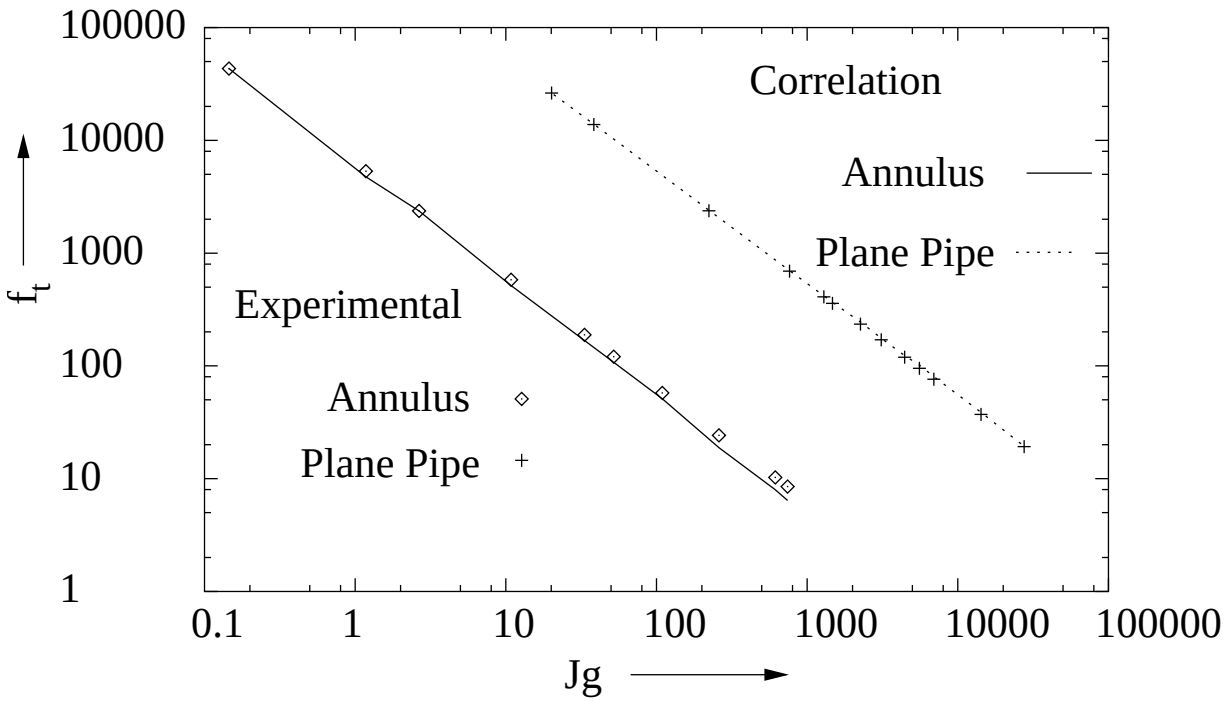

Figure 5.5: Variation of total friction factor f_t with Jg in large hydraulic diameter pipe and annulus.

plotted in Fig. 5.3. It is observed that the value of Jg is large for fluids with large values of kinematic viscosity and vice versa. Hence the hydrostatic friction factor f_{hy} is large for the fluids with small values of kinematic viscosity. Therefore it can be concluded that the friction factor results correlated in terms of Reynolds number for a particular liquid will not be applicable to another liquid when the difference in kinematic viscosity values of two fluids is large.

Present results for the variation of total friction factor with Reynolds number in large hydraulic diameter annulus and pipe are shown in Fig. 5.4. The figure also shows the comparison of data obtained from the correlations developed in the present work with the present measurements. The correlation data is in good agreement with the measurements. The correlation of friction factor is as follows:

For annulus:

$$f_t = \frac{75}{Re} + \frac{6284.39}{Jg} \tag{5.1.7}$$

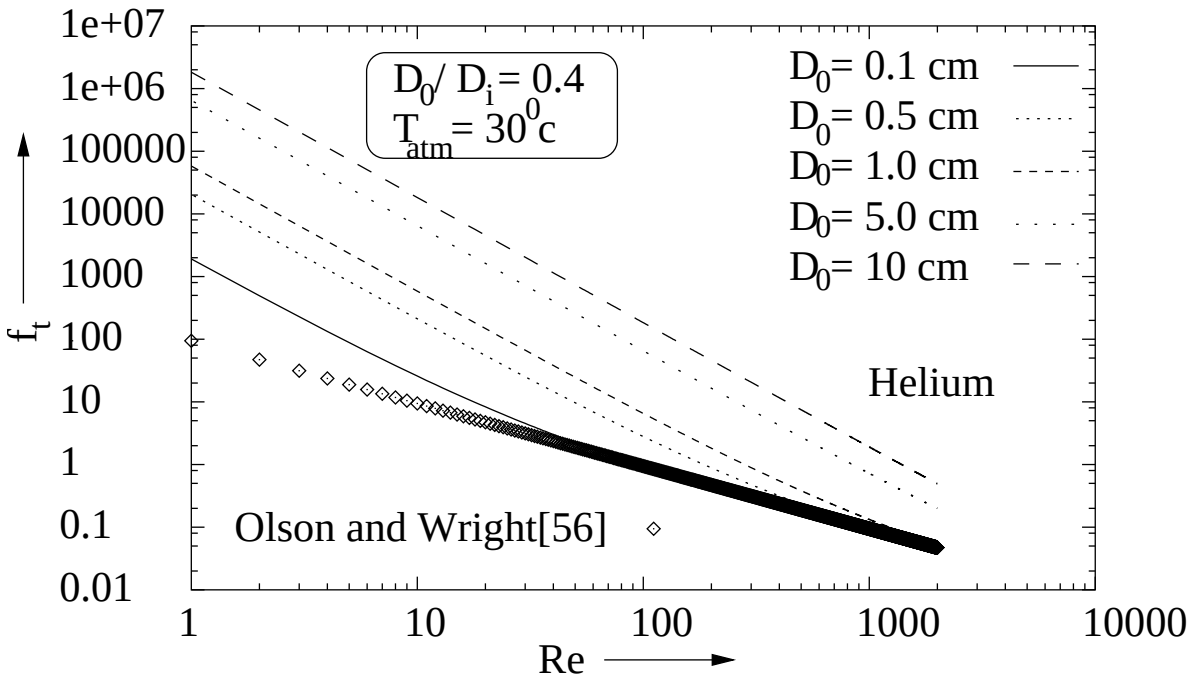

Figure 5.6: Variation of total friction factor f_t with Reynolds number Re in an annulus for different diameters with $\frac{D_i}{D_0}$ constant (=0.4) for Helium.

For plane pipe:

$$f_t = \frac{26.79}{Re} + \frac{529345.86}{Jg} \tag{5.1.8}$$

It may be observed that the value of the total friction factor is higher for plane pipe (Eq(3.2.6)) than that for the annulus (Eq3.2.7) in large hydraulic diameter ducts. The reason for large losses in plane pipe than that in annulus is that in large hydraulic diameter ducts the wall friction losses are less important compared to hydrostatic effect. More the fluid in a given cross section more the loss due to velocity gradient generated by the hydrostatic pressure. Hence in a plane pipe the values of friction factor are found to be high compared to annulus. By comparing Eq(3.2.6) and Eq(3.2.7) it can be concluded that the total friction factors in a plane pipe are more sensitive to the Jg than that in an annulus, because the value of the constant "b" for the hydrostatic friction factor is quite high in case of a plane pipe. The experimental data and correlated data for the total friction factor variation

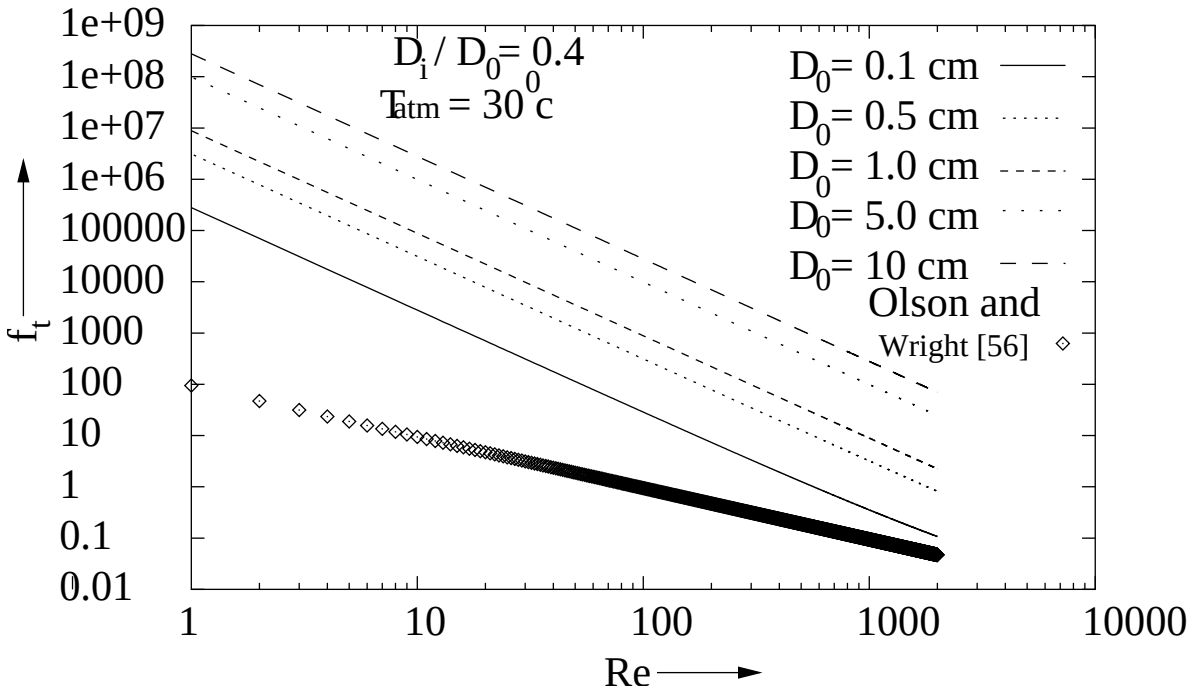

Figure 5.7: Variation of total friction factor f_t with Reynolds number Re, in an annulus for different diameters keeping $\frac{D_i}{D_0}$ constant (=0.4), using the properties of water.

with Jg is plotted in Fig. 5.5. The values of friction factor obtained in the present investigation is higher then Mody [55] and Olson and Wright [56] even though the measured pressure drop is small because the term $\frac{lQ^2}{gD_hA^2}$ in Eq(3.4.11) is negligible for large hydraulic diameter ducts.

Using the Eq(5.1.7) the variation of total friction factor with Reynolds number in the annulus is plotted in Fig. 5.6 for different diameters keeping the ratio $\frac{D_i}{D_0}$ fixed at 0.4 for helium and in Fig. 5.7 for water at 30^0 c. From figures. 5.6 and 5.7 it is clear that the results using the present correlation are in good agreement with that reported by Olson and Wright [56] only when the outer diameter is small ($D_0 \leq 0.5$ cm) and Reynolds number is large ($Re \geq 100$). The reason for this behavior is that under this condition the dynamic pressure dominates over the hydrostatic pressure, hence the high dynamic pressure nullifies the generation of velocity gradient by the

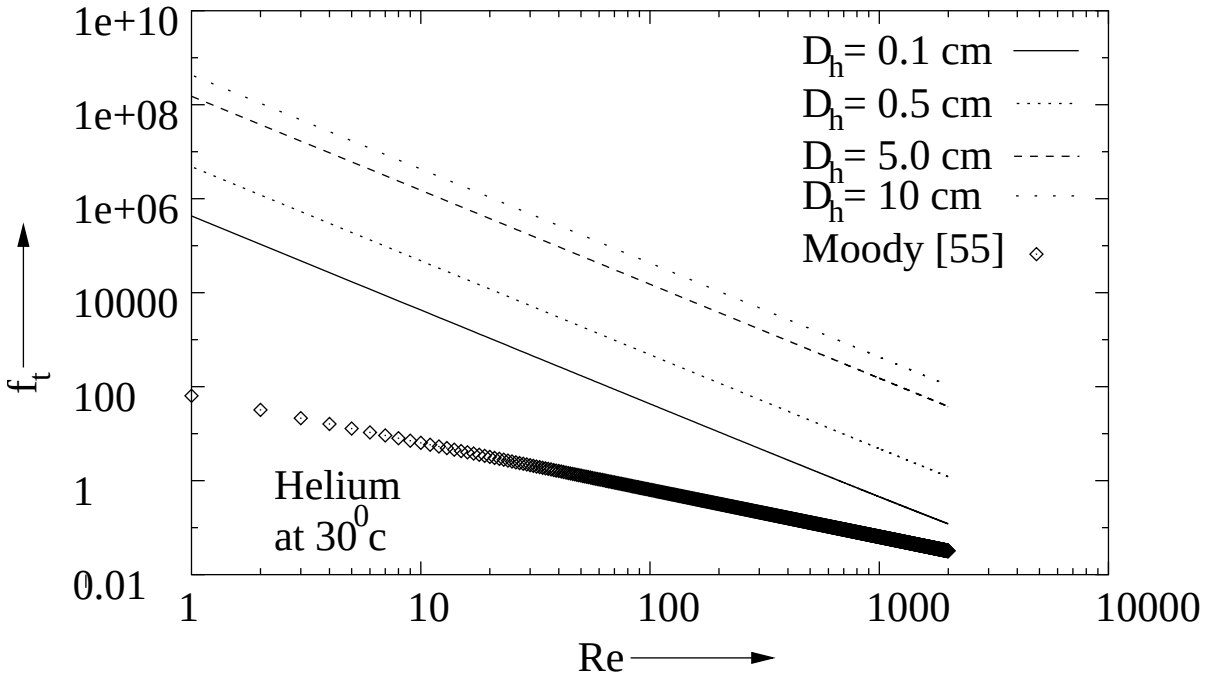

Figure 5.8: Variation of total friction factor f_t with Reynolds number Re, in a plane pipe for different diameters, using the properties of Helium He.

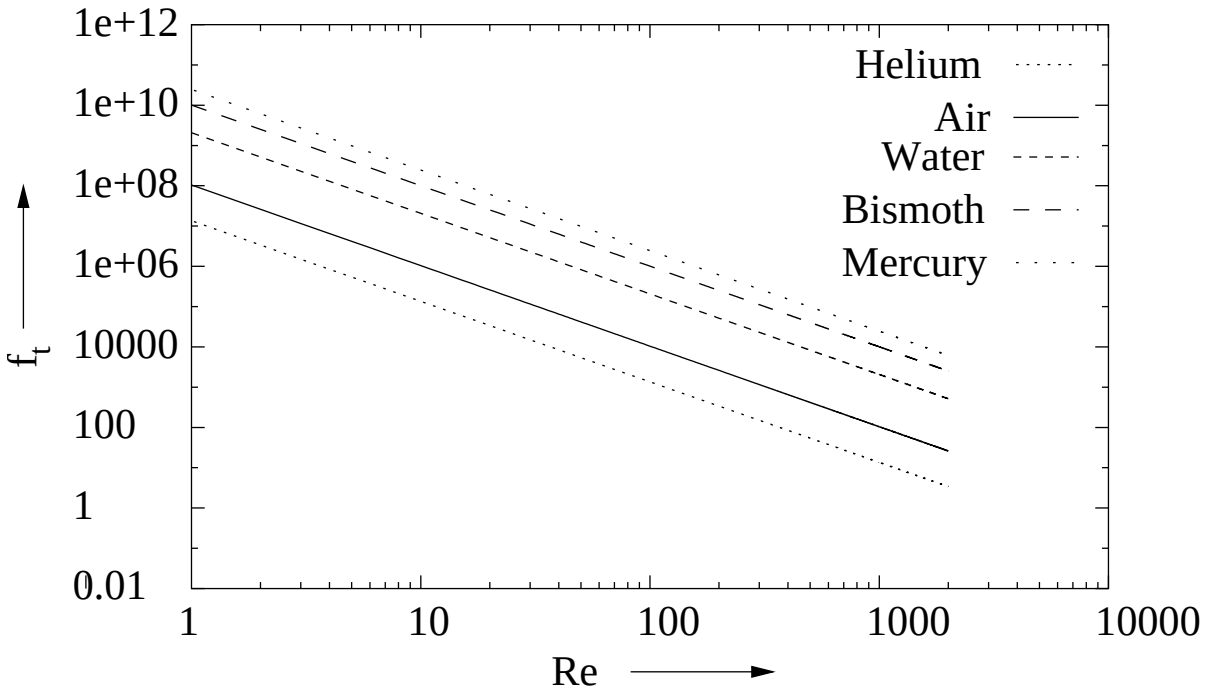

Figure 5.9: Variation of total friction factor f_t with Reynolds number Re, in a plane pipe for different liquids.

hydrostatic pressure. However it can be observed that the results for helium are in good agreement compared to that for water because water has a higher value of kinematic viscosity compared to helium.

Using the Eq(5.1.8) the variation of total friction factor with Reynolds number in plane pipe is plotted in Fig. 5.8 for different diameters for helium at 30^0 c. The observation from this figure is similar to that for Fig. 5.6. The values of friction factor are approaching to those reported by Moody [55] with a decrease of the hydraulic diameter and an increase of Reynolds number.

The variation of the total friction factor with Reynolds number for different liquids is plotted in Fig. 5.9 for plane pipe keeping diameter fixed at 3 cm. It can be seen from the figure that the values of friction factor are quite high for liquids with small values of the kinematic viscosity because for small kinematic viscosity liquids the value of Jg is negligible. As the hydrostatic friction factor is inversely proportional to Jg, the total friction factor for small kinematic viscosity liquids is quite high.

5.1.1 Conclusions

The following conclusions are drawn from the aforementioned results:

1. The hydrodynamics of flow in large diameter ducts is quite different from that in small diameter ducts, because in the former the hydrostatic pressure plays a significant role.
2. Compared to the dynamic pressure effects the hydrostatic effects are not significant for large values of Reynolds number and small hydraulic diameter ducts.
3. The hydrostatic friction factor increases with an increase in hydraulic diameter. Hence the total friction factor is quite large in large diameter ducts.

4. The correlation developed in the present work for large diameter ducts shows good agreement with that reported in the literature when the hydraulic diameter is small and the values of Reynolds number is large because at such situations the dynamic pressure dominates over the hydrostatic pressure.
5. Friction factor correlated in terms of Reynolds number for a particular fluid is not applicable to another fluid when the difference in kinematic viscosity of two fluids is large.
6. The developed correlations for friction factor as a function of Reynolds number Re and Jg is applicable for any Newtonian fluid flow in a duct.
7. The friction factors for plane pipe are larger than that for annulus in large hydraulic diameter ducts because the hydrostatic pressure drop dominates over the wall friction losses.

5.2 Study of Friction Factor in Large Diameter Annulus Using Various Configurations of Twisted Tape

A series of experiments were carried out to study the friction factor in a large hydraulic diameter annulus with various insert parameters and different number of twisted tapes in an annulus for the fully developed laminar flow. The laminar flow with varying Re from 40 to 2000 has been chosen because the hydrostatic effects are important when the Reynolds number is small. Twisted tapes of two different twist ratios $Y = 8.67$ and 9.23 and two different lengths l_{tt}=62 cm and 30 cm were used in the study.

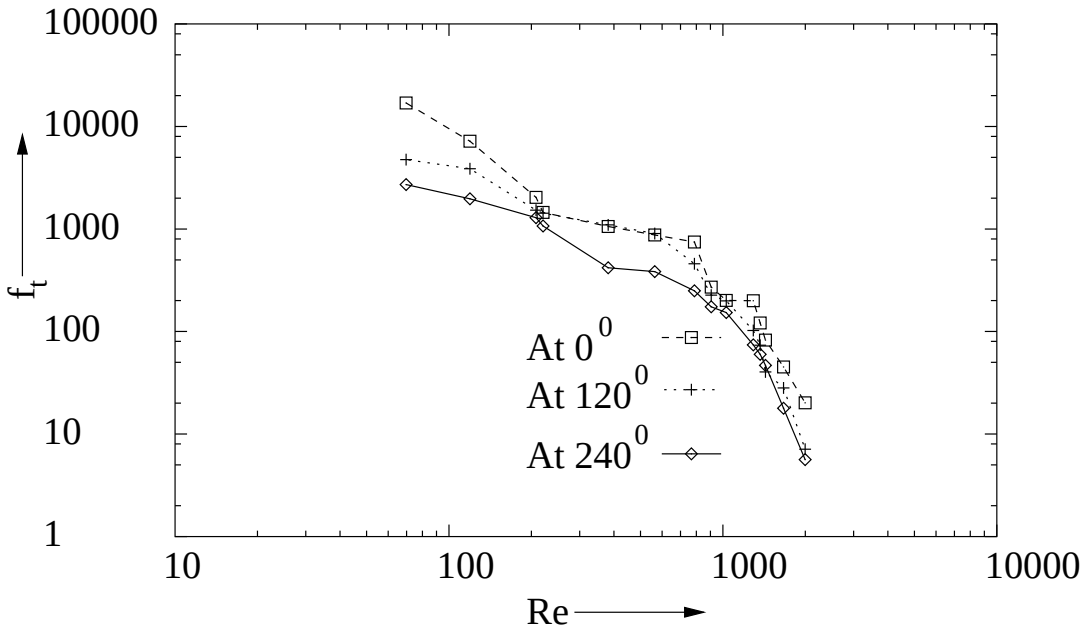

Figure 5.10: Variation of friction factor f with Reynolds number Re in an annulus with single twisted tape ($Y = 8.67$ and $l_{tt} = 62\ cm$) insert along 120^0 in streamwise direction.

Fig. 5.10 shows the variation of f with Re for a single twisted tape insert ($Y = 8.67$ and $l_{tt} = 62\ cm$) at 120^0 along the test section. It is clear that the friction factor varies in the circumferential direction, and thus the pressure drop

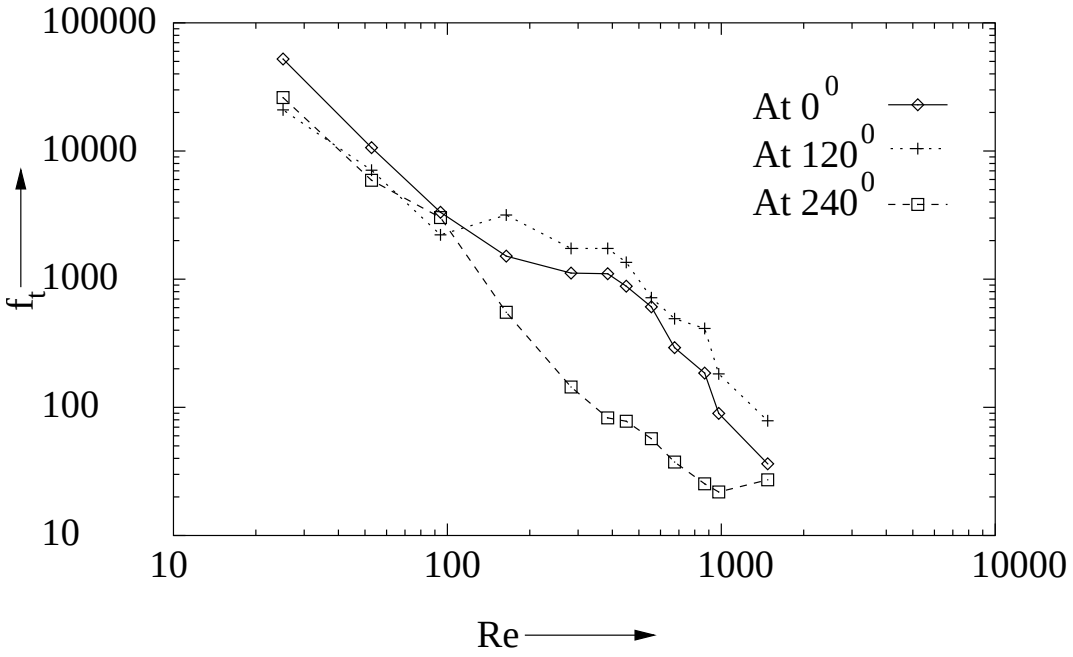

Figure 5.11: Variation of friction factor f with Reynolds number Re in an annulus with single twisted tape ($Y = 9.23$ and $l_{tt} = 30\ cm$) insert along 120^0 in streamwise direction.

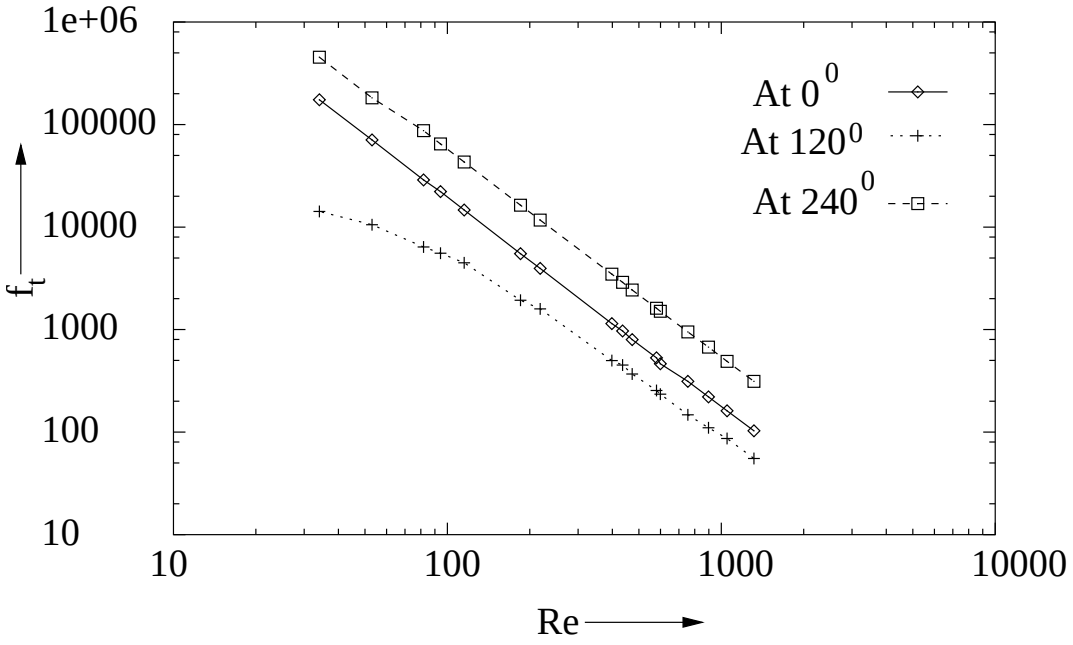

Figure 5.12: Variation of friction factor f with Reynolds number Re in an annulus with two twisted tapes ($Y = 9.23$ and $l_{tt} = 30\ cm$) insert along 120^0 and 240^0 in streamwise direction.

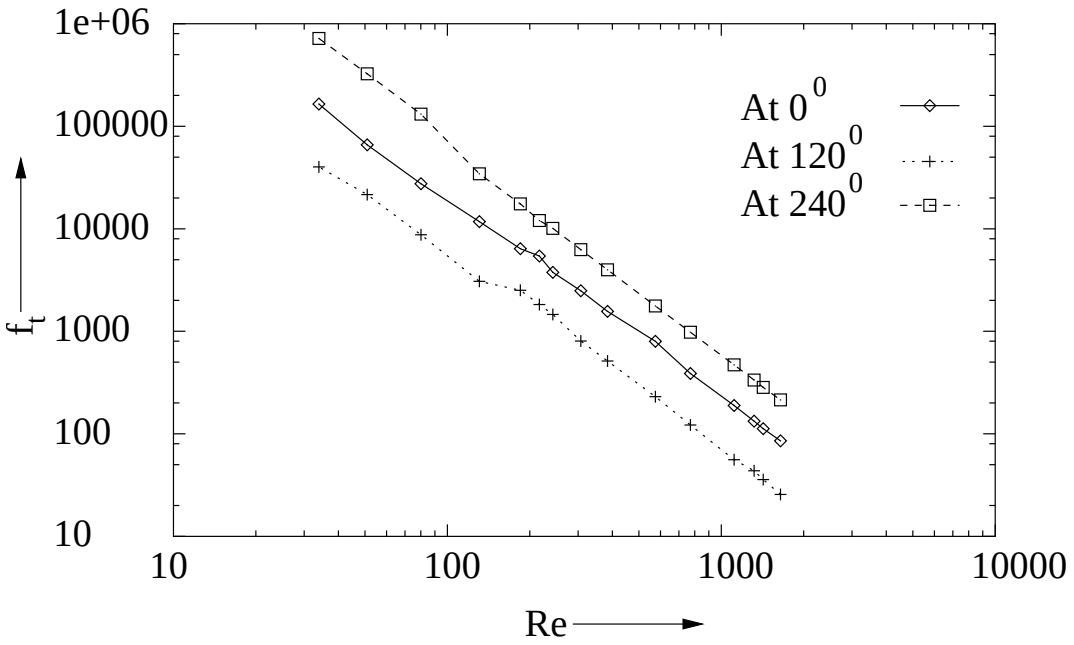

Figure 5.13: Friction factor f variation with Reynolds number Re in an annulus with three twisted tapes ($Y = 9.23$ and $l_{tt} = 30\ cm$) insert along 0^0, 120^0 and 240^0 respectively.

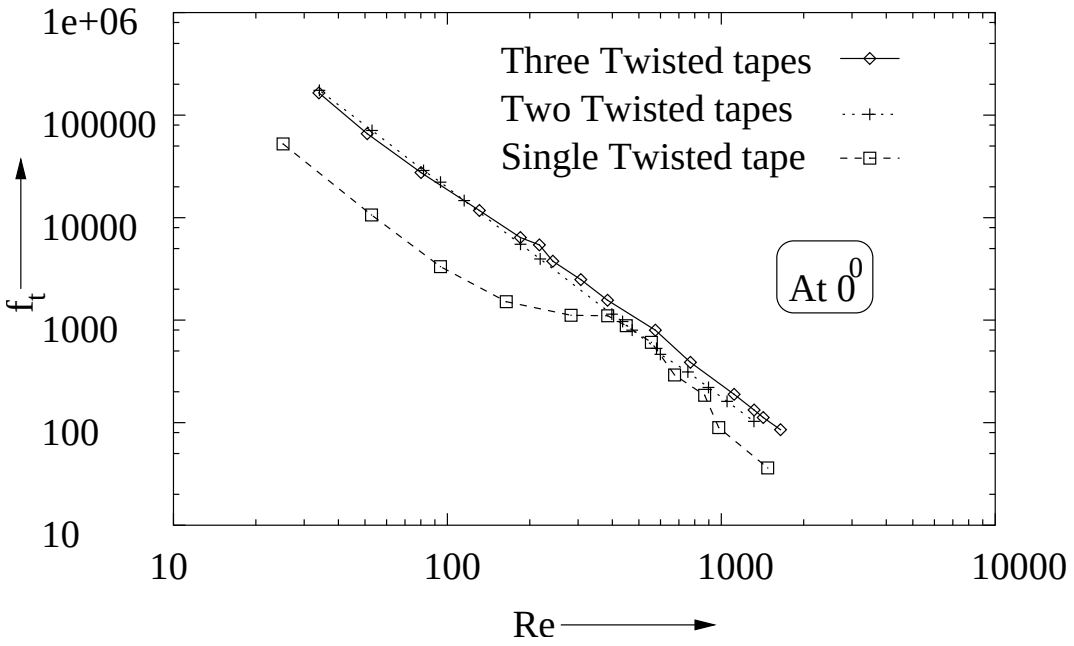

Figure 5.14: Comparison of friction factor f with Reynolds number Re for different number of twisted tapes at 0^0.

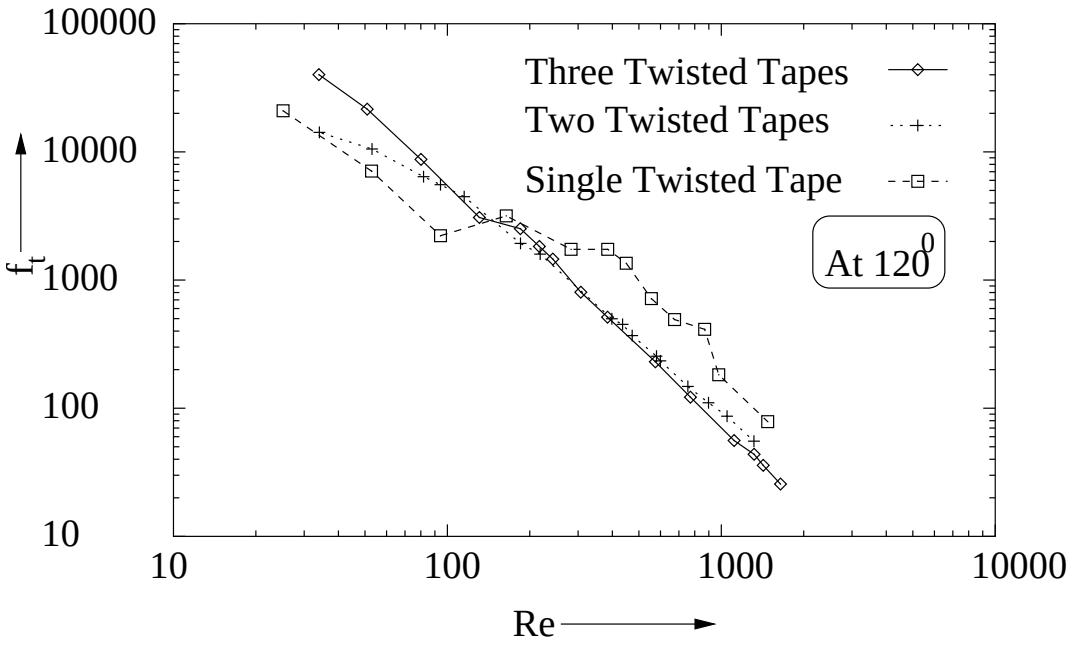

Figure 5.15: Comparison of friction factor f with Reynolds number Re along 120^0 for different twisted tapes.

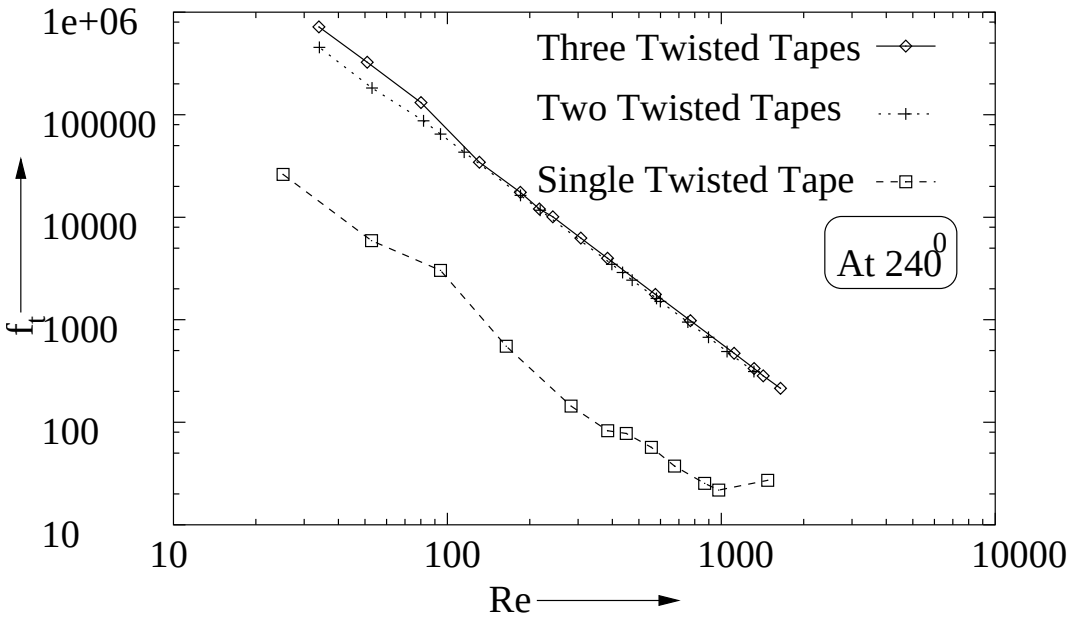

Figure 5.16: Comparison of friction factor f with Reynolds number Re along 240^0 for different number of twisted tapes.

also varies along the circumference. Fig. 5.10 further shows that the pressure drop is large along the direction of the twisted tape, and f is not a constant function of

Reynolds number along the circumference of the duct.

The variation of friction factor with Re for a single twisted tape insert ($Y = 9.23$ and $l_{tt} = 30\ cm$) at 120^0 along the test section is plotted in Fig. 5.11. The pressure drop is large along 0^0 in low Reynolds number range ($Re < 100$) and as Reynolds number increases, the pressure drop along the 120^0 exceeds that along 0^0. The pressure drop along 240^0 is found to be small for all the values of tested Reynolds number.

The variation of friction factor with Reynolds number for two twisted tape inserts ($Y = 9.23$ and $l_{tt} = 30\ cm$) at 120^0 and 240^0 along the test section is shown in Fig. 5.12. It is observed that except for the small values of Reynolds number the friction factor along 120^0 varies almost linearly with Reynolds number throughout the tested range.

Figure. 5.13 shows the variation of friction factor with Reynolds number for three twisted tapes inserts ($Y = 9.23$ and $l_{tt} = 30\ cm$) at 120^0, 240^0 and 0^0 along the test section. Here the friction factor is found to vary almost linearly along the three angles considered. However the pressure drop is found to be highest at 240^0 along the test section, followed by that for 0^0 and 120^0.

The comparison for friction factor variation along 0^0 for single, two, and three twisted tapes inserts ($Y = 9.23$ and $l_{tt} = 30\ cm$) is shown in Fig. 5.14. It is found that the friction factors for the three twisted tape inserts is quite high compared to the single twisted tape insert throughout the tested Reynolds number range. However the difference in the friction factor for two twisted tape and three twisted tape insert is found to be insignificant.

Figure. 5.15 represents the variation of friction factor at 120^0 along the test section for single, two and three twisted tapes inserts ($Y = 9.23$ and $l_{tt} = 30\ cm$)

along the test section. Here it is observed that for $Re < 300$, the values of friction factor are quite high for the three twisted tapes inserts followed by the single twisted tape and two twisted tape inserts respectively. When $Re > 300$ the friction factor for single twisted exceeds than that for two and three twisted tape inserts. Further it is observed that the friction factor for the two and three twisted tape insert is almost same when $Re > 300$.

A comparison of friction factor variation along 240^0 for single, two and three twisted tapes ($Y = 9.23$ and $l_{tt} = 30\ cm$) insert is plotted in Fig. 5.16. It can be easily pointed out that the values of friction factor for three and two twisted tape inserts are almost same, whereas the values of friction factor for the single twisted tape insert are found to be much smaller in comparison to the other two cases.

5.2.1 Conclusions

For large hydraulic diameter annulus with twisted tape inserts the following conclusions may be drawn:

1. The friction factor varies circumferentially.
2. The friction factor is not a constant function of Reynolds number.
3. The friction factor increases with increase in number of inserts, however the increment in friction factor from two twisted tape inserts to three twisted tape inserts is not significant.
4. The friction factor is found to be large along the twisted tape insert.

5.3 Heat Transfer Study in a Large Hydraulic Diameter Annulus

Experiments were carried out for different values of heat flux to study the variation of Nusselt number with Reynolds number in a large diameter annulus without and with insert. Single twisted tape of dimension $Y = 9.23$ and $l_{tt} = 30\ cm$ was inserted at the leading edge of the test section along the 0^0. The the Nusselt number variation along the stream wise direction is studied. All the experiments are carried out under steady state condition. The detailed discussion of the results is as follows:

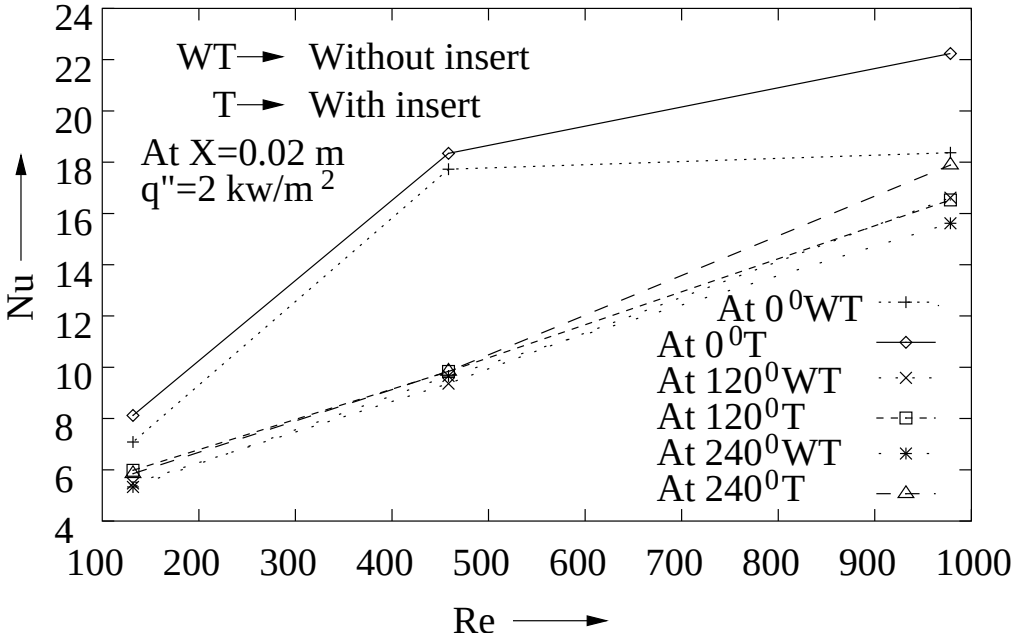

Figure 5.17: Comparison of circumferential variation (at 0^0, 120^0 and 240^0) of Nusselt number as a function of Reynolds number at X=0.02 m for uniform heat flux q"=2 $\frac{kw}{m^2}$, with and with out twisted tape insert.

Figs. 5.17, 5.18 and 5.19 show the circumferential variation of Nusselt number with Reynolds number for different input heat fluxes with and without twisted tape insert (at 0^0). It can be seen that the Nusselt number increases with Reynolds number for both with and without the twisted tape insert. It is found that the increase of Nusselt number due to twisted tape insert is high along the twisted tape

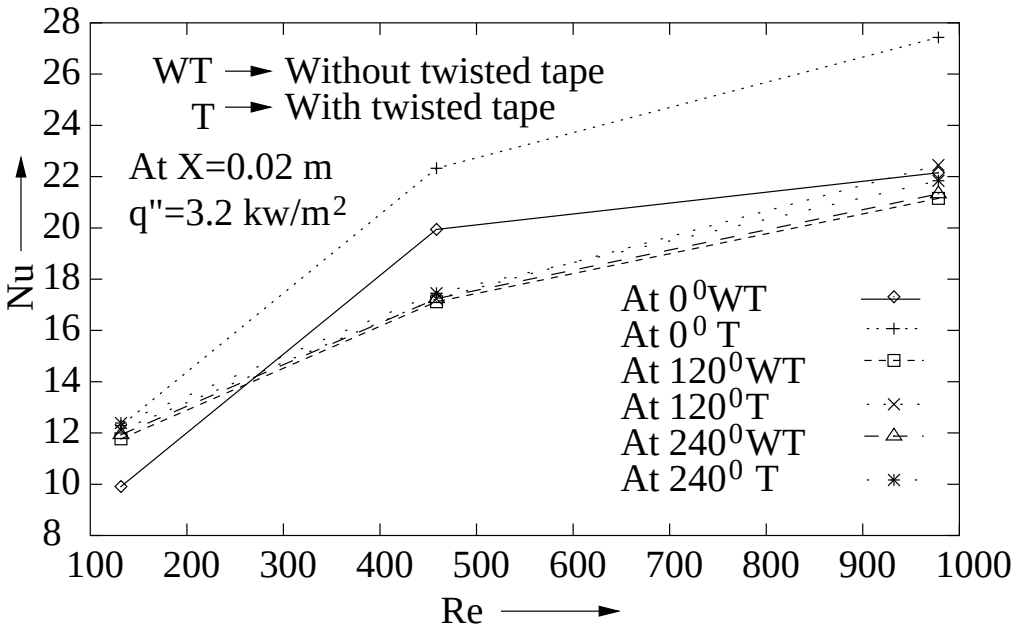

Figure 5.18: Comparison of circumferential variation (at 0^0, 120^0 and 240^0) of Nusselt number as a function of Reynolds number at X=0.02 m for uniform heat flux q"=3.2 $\frac{kw}{m^2}$, with and with out twisted tape insert.

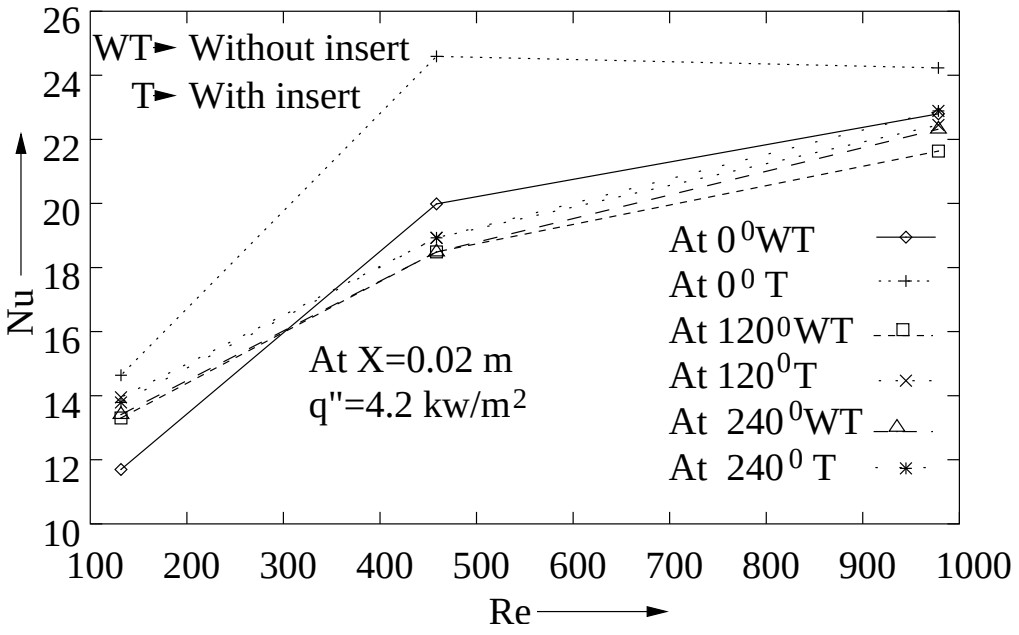

Figure 5.19: Comparison of circumferential variation (at 0^0, 120^0 and 240^0) of Nusselt number as a function of Reynolds number at X=0.02 m for uniform heat flux q"=4.2 $\frac{kw}{m^2}$, with and with out twisted tape insert.

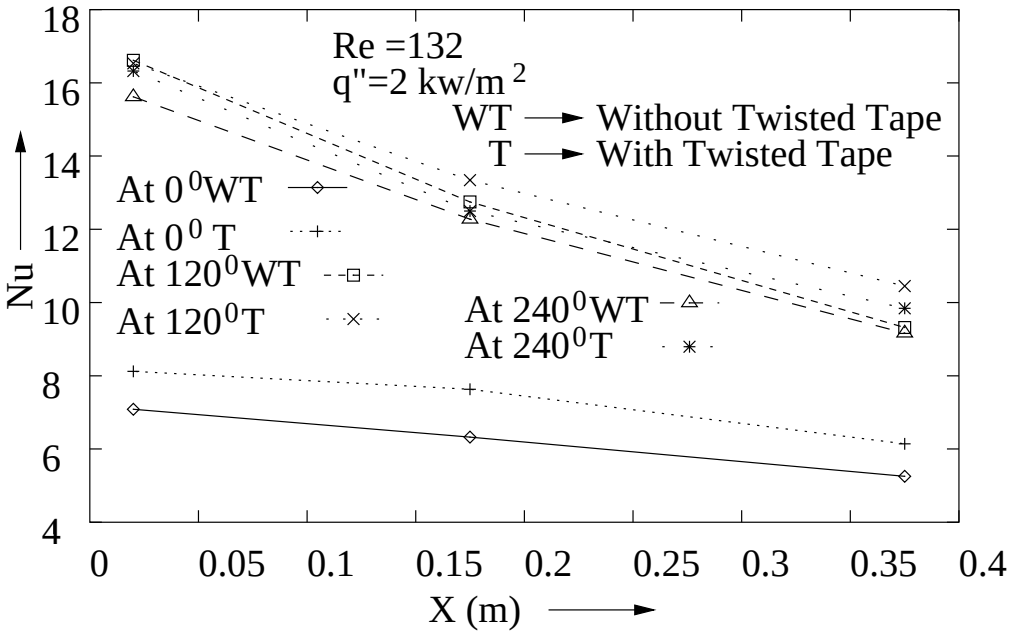

Figure 5.20: Comparison of circumferential variation (at 0^0, 120^0 and 240^0) of Nusselt number as a function of distance from the leading edge of test section (X=0 m), for uniform heat flux q"=2 $\frac{kw}{m^2}$, with and with out twisted tape insert.

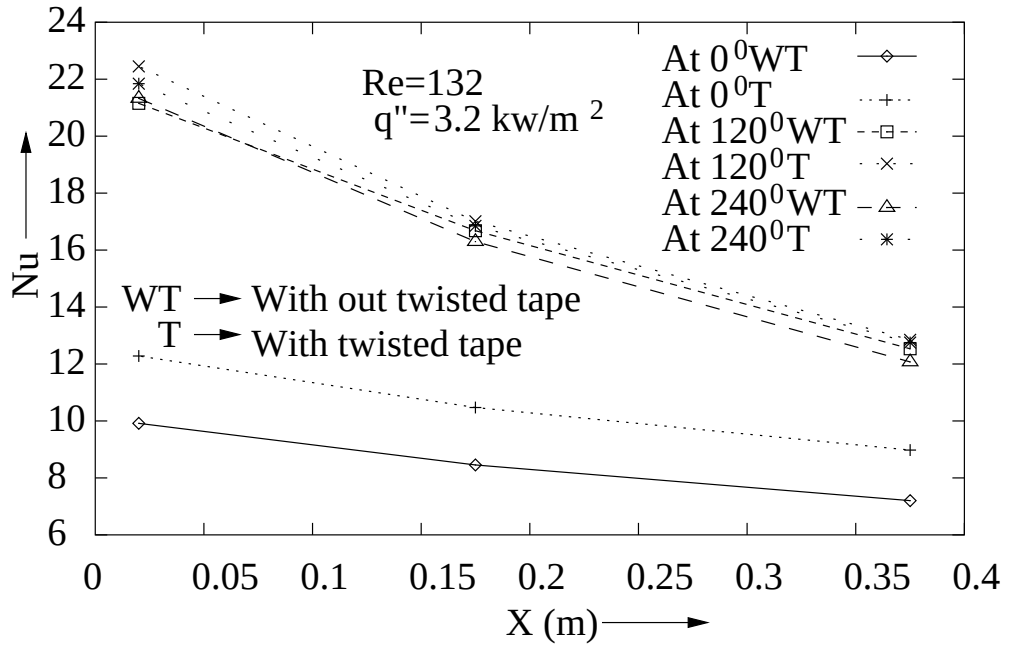

Figure 5.21: Comparison of circumferential variation (at 0^0, 120^0 and 240^0) of Nusselt number as a function of distance from the leading edge of test section (X=0 m), for uniform heat flux q"=3.2 $\frac{kw}{m^2}$, with and with out twisted tape insert.

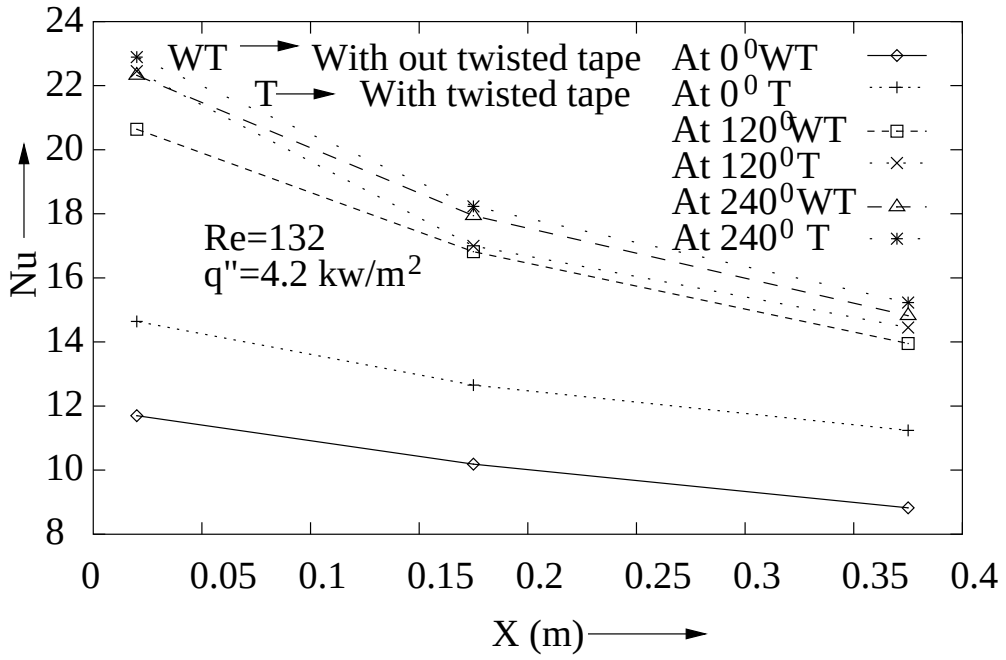

Figure 5.22: Comparison of circumferential variation (at 0^0, 120^0 and 240^0) of Nusselt number as a function of distance from the leading edge of test section (X=0 m), for uniform heat flux q"=4.2 $\frac{kw}{m^2}$, with and with out twisted tape insert.

insert (along 0^0). The increase in Nusselt number along other two angles (120^0 and 240^0) is found to be negligible. It can be seen from the figures (5.17, 5.18, 5.19) that the increase in Nusselt number due to insert is large for high Reynolds number. The reason for this is that the swirl flow generated by the twisted tape dies up quickly for small Reynolds number due to lack of dynamic pressure or inertia force.

Figures. 5.20, 5.21 and 5.22 show the variation of Nusselt number with distance from the leading edge of the test section for different values of the input heat flux. It is observed that the Nusselt number decreases with an increase in distance from the leading edge. This is because the bulk fluid temperature increases along the test section. It is also observed that the increase in Nusselt number due to twisted tape insert is more at the leading edge of the test section, but it goes on reducing in the downstream direction. This nature of Nusselt number variation is due to decay of swirl flow along the downstream of the test section.

Chapter 6

CONCLUSIONS AND FUTURE SCOPE

6.1 Conclusions

The following conclusions are drawn from the present study:

1. The flow pattern in a small hydraulic diameter duct ($D_h \geq 30\ mm$) is different from that in a large diameter duct.
2. In a large diameter duct the pressure loss is found to be less dependent on the wall friction as compared to the loss due to the hydrostatic effect.
3. In a large diameter pipe the velocity profile also depends on the hydrostatic pressure variation along the radial direction.
4. The hydrostatic friction factor increases with an increase in the hydraulic diameter.
5. The results obtained in the literature for small hydraulic diameter pipes as a function of Reynolds number cannot be applicable to large diameter pipes because in large diameter pipes hydrostatic pressure also plays a significant role.
6. The values of the friction factor in large hydraulic diameter pipe and annulus are found to be more than those reported in the literature.

7. The variation of the friction factor along the circumferential direction in a large diameter pipe and annulus without any insert are found to negligible in the present experimental work.
8. With the twisted tape insert in a large hydraulic diameter annulus friction factor is found to be significant along the circumferential direction.
9. The Nusselt number in a large hydraulic diameter annulus is found to vary circumferentially for both with and without insert.
10. A significant increase in Nusselt number is noted along the twisted tape insert for large Reynolds number at the leading edge of the test section.
11. The results from the present work will be useful in the design of large diameter duct systems.

6.2 Future Scope

The study of fluid mechanics and heat transfer in a large diameter ($D_h \geq 30\ mm$) is a active area of research. It is found that a limited literature is available in this area. Hence there is a scope for research in this area. The following area may be suggested for further study in large diameter ducts:

1. The velocity distribution for a fully developed flow inside a large hydraulic diameter duct can be studied for fluids with different values of the kinematic viscosity.
2. The friction factor can be correlated as a function of Reynolds number Re, a parameter Jg representing hydrostatic pressure, circumferential variation θ, twist ratio Y and the length of the twisted tape for the flow in a large hydraulic diameter duct with different twisted tape inserts.
3. Heat transfer study can be done with various inserts like twisted tape wire coils, porous medium and ribs, for different fluids.

4. The Nusselt number can be correlated as a function of Reynolds number, a parameter Jg representing hydrostatic pressure, circumferential variation θ, twist ratio Y, length of twisted tape and the Prandtl number for the flow in a large hydraulic diameter duct with different twisted tape inserts.
5. The effect of hydrostatic pressure on the developing length in a internal flow can be studied.
6. Using the computational method the different fluid mechanics and heat transfer parameters can be studied for a flow in a large diameter duct.
7. To optimize the performance of a heat exchanger with a large hydraulic diameter, a complete thermodynamic analysis can be suggested to minimize the entropy generation.

REFERENCES

1. Bergles, A.E., (1985), Techniques to augment Heat Transfer, Handbook of Heat Transfer Applications, ed., Rohsenow, W.M., et.al., Chapter 3, McGraw Hill, New York.

2. Witham, J.M. (1896), The effects of retarders in fire tubes of steam boilers, Street Railway J, Vol. 12, No. 6, p 374.

3. Royds, R. (1921), Heat transmission by radiation, conduction and convection, Constable and Camp Ltd., London, 1^st ed., pp. 190-201.

4. Cresswell, J.D. (1958), Mechanics of swirling turbulent flow, M.S. thesis, Lehigh University, U.S.A.

5. Kreith, F. and Margolis, D. (1959), Heat transfer and friction in turbulent vortex flow, App. Sc. Res., Section A, Vol. 8, No. 6, pp. 457-473.

6. Thorsen, R. and Landis, F. (1968), Friction and heat transfer characteristics in tubular swirl flow subjected to large transverse temperature gradients, ASME J Heat Transfer, Vol. 90, No. 1, pp. 87-97.

7. Gambill, W.R. and Bundy, R.D. (1963), High flux heat transfer characteristics in turbulent swirl flow subjected to large transverse temperature gradients, AIChE J, Vol. 9, No. 1, pp. 55-59.

8. Smithberg, E. and Landis, F. (1964), Friction and forced convection heat transfer characteristics in tubes with twisted tapes swirl generations, ASM J Heat Transfer, Vol. 86, No. 1, pp. 39-49.

9. Lopina, R.F. and Berrgles, A. E. (1969), Heat transfer and pressure drop in tape-generated swirl flow of single-phase water, ASME J Heat Transfer, Vol. 91, No. 3, pp. 434-441.

10. Colburn, A.P. and King, W. J. (1931), Heat transfer and pressure drop in empty, baffled and packed tubes, III, Relation between heat transfer and pressure drop, Industrial Engg. Chemistry, Vol. 23, No. 8, pp. 919-923.

11. Seigel, L.G. (1946), The effect of turbulence promoters on heat transfer coefficients of water flowing in a horizontal tube, Heating, piping and Air Conditioning, Vol. 18, No. 6, pp. 111-114.

12. Koch, R. (1958), pressure loss and heat transfer for turbulent flow, VDI-forschungsheft, Vol. 24, No. 469. ser. B, pp. 1-44.

13. Seymour, E.V. (1963), A note on the improvement in performance obtainable from fitting twisted-tape turbulence promoters to tubular heat exchangers, JIchE, Vol. 41, No. 4, pp. 159-162.

14. Kreith, F. and Sonju, O.K., (1965), The decay of a turbulent swirl flow in a pipe, J Fluid Mechanics, Vol.22, part 2, pp. 257-271.

15. Date, A.W. (1973), Flow in tubes containing twisted tapes, Heating and Ventilation Engineer, J Environmental Sciences, Vol. 47, No. 556, pp. 240-249.

16. Klepper, O.H. (1972), Heat transfer performance of short twisted tapes, AIChE, paper No. 35, Aug 6-9, 24p.

17. Kidd Jr., G.J. (1969), Heat transfer and pressure drop for nitrogen flowing in tubes containing twisted tapes, AIChE J, Vol. 15, No. 4, pp. 581-585.

18. Date, A.W. (1974), Prediction of fully developed flow in a tube containing a twisted- tape, Int. J Heat Mass Transfer, Vol. 17, No. 8, pp. 845-859.

19. Bolla, G., De Giorgio, G. and Pedrocchi, E. (1973), Heat transfer and pressure drop comparison in tubes with transverse ribs and with twisted-tapes, Energia Nuclear (Milan), Vol.20, No. 11, pp. 604-613.

20. Zozulya, N.V. and Shkuratov, I.Y. (1974), Effect of length of twisted tape turbulence promoter and its initial twisting pitch on augmentation of heat transfer inside a tube, Heat Transfer Soviet Research, Vol.6, No. 6, pp. 98-100.

21. Huang, F. and Tsou, F.K. (1979), Friction and heat transfer in turbulence free swirling flow in pipes, ASME paper 79-HT-39, 9p.

22. Blackwelder, R. and Kreith, F. (1970), Experimental investigation of heat transfer and pressure drop in a decaying swirl flow, ASME, Augmentation of Convective Heat and Mass Transfer, pp. 102-108.

23. Backshall, R.G. and Landies, F. (1969), Boundary layer velocity distribution in turbulent swirl pipe flow, ASME paper No., 69- FE - 14, 6p.

24. Watanabe, K., Taira, T. and Mori, Y. (1983), Heat transfer augmentation in turbulent flow by twisted tapes at high temperatures and optimum performance, Heat Transfer-Japanese Research, Vol.12, No. 3, pp. 1-31.

25. Genis, G.J. and Rautenbach, W.L. (1987), High heat flux, forced convection heat transfer for tubes with twisted tape inserts, ASME, HTD, Vol. 68, pp. 1-9.

26. Budov, V.M., Zamyatin, S.A. and Farafonov, V.A. (1985), Distribution of velocity and pressure in a cylindrical channel with flow swirled by local twisted-tape swirls, Thermal Engineering, Vol. 32, No. 9, pp. 520-521.

27. Beckermann, C. and Goldschmid, V.W. (1986), Heat transfer augmentation in the flueway of a water heater, ASHRAE trans., Vol. 92, pt. 2B, pp. 485-495.

28. Yamada, Y., Akai, M. and Mori, Y. (1984), Shell and tube side heat transfer augmentation by the use of wall radiation in a cross flow shell and tube heat exchanger, ASME J Heat Transfer, Vol. 106, No.4, pp. 735-742.

29. Gupte, N.S. and Date, A.W. (1989), Friction and heat transfer characteristics of helical turbulent air flow in annuli, ASME J Heat Transfer, Vol. 111, pp. 337-344.

30. Filipak, E. (1980), Heat transfer in a vertical tube with twisted-tape swirl generators, Zeszyty Naukowe Politechniki Lodzkiej Mechanika, No. 60, pp. 41-53.

31. Donevski, B. and Kulesza, J. (1980), Friction during isothermal turbulent flow in tubes with twisted-tape, Zeszyty Naukowe Politechniki Lodzkiej Mechanika, No. 58, pp. 5-25.

32. Rao, K.S. (1983), Augmentation of heat transfer in the axial ducts of electrical machines with tape generated swirl flow, IEEE Trans. On Power Apparatus and Systems, Vol. PAS- 102, No. 8, pp. 2750-2756.

33. Fomina, V.N., Fedorov, I.I., Titova, E.Y., Martynychev, M.I. and Romanov, A.I. (1987), Thermal efficiency and operational reliability of finned-tube economizers of p-57-3M boilers, Thermal Engineering, Vol. 34, No. 5. pp. 250-253.

34. Algifri, A.H. and Bharadawj, R.K. (1985), Prediction of heat transfer for decaying turbulent swirl flow in a tube, Int. J Heat Mass Transfer, Vol. 28, No. 9, pp. 1637-1643.

35. Algifri, A.H. and Bharadawj, R.K. and Rao, Y.V.N. (1988), Heat transfer in turbulent decaying swirl flow in a circular pipe, Int. J Heat Mass Transfer, Vol. 31, No. 8, pp. 1563-1568.

36. Burfoot, D. and Rice, P. (1983), Heat transfer and pressure drop characteristic of short lengths of swirl flow inducers inter spacing along a circular duct, Chemical Engg. Research and Design, Vol. 61, No. 4, pp. 253-258.

37. Kumar, R. and Bharadwaj, R.K. (1979), Heat transfer and pressure drop in decaying swirl flow of water through a tube containing the twisted-tape, J Inst. Engineers (India), part MC, Mech. Engg. Div., Vol. 60, pt ME 2, pp. 72-77.

38. Kumar, A. and Prasad, B.N. (2000), Investigation of twisted-tape inserted solar water heater heat transfer, friction factor and thermal performance results, Renewable Energy, Vol. 19, No. 3, pp. 379-398.

39. Fujita, Y. and Lopez, A.M. (1995), Heat transfer enhancement of twisted inserts in turbulent pipe flows, Heat Transfer- Japaneses Research, Vol. 24, No. 4, pp. 378-396.

40. AI-Fahed, S. and Chakroun, W. (1996), Effect of tube-tape clearance on heat transfer for fully developed turbulent flow in a horizontal isothermal tube, Int. J Heat and Fluid Flow, Vol. 17, No. 2, pp. 173-178.

41. Saha, S.K., Gaitonde, U.N. and Date, A.W. (1990), Heat transfer and pressure drop characteristic of turbulent flow in a circular tube fitted with regularly spaced twisted-tape elements, Experimental Thermal and Fluid Science, Vol. 3, No. 6, pp. 632-640.

42. Rao, M.M. and Sastri, V.M.K. (1995), Experimental investigation for fluid flow and heat transfer in a rotating tube twisted tape inserts, Int. J Heat Transfer Engineering, Vol. 16, No. 2, pp. 19-28.

43. Manglik, R.M. and Bergles, A.E. (1993), Heat transfer and pressure drop correlations for twisted-tape insert in isothermal tubes, Part II-Transition and turbulent flows, ASME J Heat Transfer, Vol. 115, No. 4, pp. 890-896.

44. Sivanshanmugam, P. and Sunduram, S. (1999), Improvement in performance of heat exchanger fitted with twisted tape, J Energy Engg., Vol. 125, No. 1, pp. 35-40.

45. Agarwal, S.K. and Raja Rao, M. (1996), Heat transfer augmentation for the flow of viscous liquid in circular tubes using twisted tape inserts, Int. J Heat Mass Transfer, Vol. 39, pp. 3547-3557.

46. Peterson, S.C., France, D.M. and Carlson, R.D. (1989), Experiments in high pressure turbulent swirl flow, ASME, HTD, Vol. 108, pp. 215-218.

47. Numov, V.K. and Semashko, N.N. (1994), Analytical model of estimating thermo-physical and strength parameters of cooled pipe with the twisted tape under asymmetric heating by a pulse of external heat flux, Plasma Devices and Operations, Vol. 3, No. 4, p. 267.

48. Naumov, V.K., Semashko, N.N. and Komov, A.T. (1995), Finite difference approximation of the adiabatic cross section technique in a numerical analysis of single side heating process of a cooled pipe with twisted tape inside by a external heat flux pulse, Plasma Devices and Operations, Vol. 4, No. 2, p. 141.

49. Naumov, V.K., Semashko, N.N. and Komov, A.T. (1995), Modification of adiabatic cross section technique for calculation of pipes containing twisted tapes under asymmetric heating by a external stationary heat flux with a high power density, Plasma Devices and Operations, Vol. 5, No. 1, pp. 43-58.

50. Yokoya, S., Takagi, S., Lguchi, M., Marukawa, K., Yasugaira, W. and Hara, S. (2000), Development of swirling flow generator in immersing nozzle, ISIJ Int., Vol. 40, No. 6, pp. 584-588.

51. Klaczak, A. (1996), Heat transfer and pressure drop in tubes with short turbulators, Waerme-und Stoffuebertragung, Vol. 31, No. 6, pp. 399-401.

52. Hijikata, K., Nagasaki, T. and Minami, K. (1994), Study of heat transfer augmentation in a high-temperature field by a radiation promoted generating a secondary flow, Int. J Experimental Thermal and Fluid Science, Vol. 7, No. 1, pp. 31-42.

53. Saha, S.K. and Dutta. A. (2001), Thermo hydraulic study of laminar swirl flow through a circular tube fitted with Twisted tapes, ASME J Heat Transfer, June 2001, Vol. 2, pp. 417-421.

54. Inaba, H. and Ozaki, K. (2001), Heat transfer enhancement and flow drag reduction of forced convection in circular tubes by means of wire coil insert, in: Shah, R.K., Bell, K.J., Mochizuki, S. and Wadekar, V.V., (Eds.). Handbook of Compact Heat Exchanger, Int, ed., pp. 445-452.

55. Moody, L.F. (1944), Friction Factors for Pipe Flow, Trans. ASME, Vol. 66, pp. 671-678.

56. Olson, R.M. and Wright, S.J. (1990), Essentials of Engineering Fluid Mechanics, Harper & Row, New York.

57. Ozisik, M.N., (1985), Heat transfer, McGrawHill Book Company, Int, ed., pp. 332-336.

58. Khurmi, R.S. and Gupta, J.K. (1997), Machine Design, Text Book, Eurasia Publishing House (Pvt) LTD, Ram Nagar, New Delhi.

59. Bhatti, M.S. and Saha, R.K. (1987), Turbulent and transition flow convective heat transfer, in: Kakac, S., Saha, R.K. and Aung, W., (Eds.). Handbook of Single-Phase Convective Heat Transfer, Chap. 4. John Wiley and Sons, New York.

60. Kline, S.J. and McClintock, F.A. (1953), Describing uncertainties in single sample experiments, Mechanical Engineering 75, pp. 3-8.

APPENDIX

A1: Error Analysis for Pressure Drop Measurements

The error involved in the measurement of the friction factor in the present experiment is calculated as suggested by Kline and McClintock [60]. The calculation is as follows:

$$f = \frac{\Delta P}{\frac{1}{2}\rho V^2[4\frac{l}{D_h}]}$$

The above equation can reduce to:

$$f = \frac{2gD_h(Head\ of\ water\ )}{4lV^2}$$

Uncertainty in the measurement of velocity of water is given by:

$$\frac{\partial V}{V} = [(\frac{\partial Q}{Q})^2 + (\frac{\partial A}{A})^2]^{1/2}$$

$$\frac{\partial A}{A} = 2(\frac{\partial D_h}{D_h})$$

Uncertainty in the measurement of the friction factor is given by:

$$\frac{\partial f}{f} = [(\frac{\partial D_h}{D_h})^2 + (\frac{\partial (Head)}{Head})^2 + (\frac{\partial l}{l})^2 + 4(\frac{\partial V}{V})^2]^{1/2}$$

The following are the uncertainties associated with the parameters:

$$Head\ of\ \ water\ \ = h \pm 1\ mm$$

$$l = 1000.25 \pm 1\ mm$$

$$Q = Q \pm 0.75\ lpm$$

$$D_h = 30 \pm 0.5\ mm$$

In the present experiments it is found that the uncertainty involved in the calculation of average velocity is around $\pm 4.2\%$. The water head available at the inlet to the

present test section for the smallest tested Reynolds number (Re=50) is 900.25 mm. Substituting the above values in the calculation of uncertainty for friction factor:

$$\frac{\partial f}{f} = [(\frac{0.5}{30})^2 + (\frac{1}{900.25})^2 + (\frac{1}{1000.25})^2 + 4(\frac{4.2}{100})^2]^{1/2} \times 100 = 8.6\%$$

Hence the estimated uncertainty in the friction factor calculation is around $\pm 9\%$.

A2: Error Analysis for Heat Transfer Measurements

The error involved in the measurement of the steady state heat transfer coefficient in the present experiment is calculated as suggested by Kline and McClintock [60]. The calculation is as follows:

$$\frac{\partial h}{h} = \sqrt{(\frac{\partial q}{q})^2 + (\frac{\partial \Delta T}{\Delta T})^2}$$

where

$$\Delta T = T_W - T_\infty$$

In the present measurements

$$q = q\ W\ \pm 3\ W$$

$$\partial \Delta T = \Delta T^0\ C\ \pm 1^0\ C\quad for\quad q = 200\ w$$

$$\partial \Delta T = \Delta T^0\ C\ \pm 2^0\ C\quad for\quad q = 100\ w$$

The uncertainty involved in heat transfer coefficient measurement for a power input of

200 W:

$$\frac{\partial h}{h} = \sqrt{(\frac{3}{200})^2 + (\frac{1}{21.04})^2} \times 100 = \pm 5\%$$

100 W:

$$\frac{\partial h}{h} = \sqrt{(\frac{3}{100})^2 + (\frac{2}{7.17})^2} \times 100 = \pm 28.05\%$$

Hence the estimated uncertainty in the heat transfer coefficient calculation is between $\pm 5\%$ - $\pm 28.5\%$.